

RESEARCH

Open Access



Cyclic soft stimulation (CSS): a new fluid injection protocol and traffic light system to mitigate seismic risks of hydraulic stimulation treatments

Hannes Hofmann^{1*} , Günter Zimmermann¹, Arno Zang² and Ki-Bok Min³

*Correspondence:
hannes.hofmann@gfz-potsdam.de
¹ Section Geothermal Energy
Systems, Helmholtz Centre
Potsdam GFZ German Research
Centre for Geosciences,
Telegrafenberg, 14473 Potsdam,
Germany
Full list of author information
is available at the end of the
article

Abstract

Hydraulic stimulation treatments are standard techniques to access geologic resources which cannot economically be exploited with conventional methods. Fluid injection into unproductive formations may increase their permeability by forming new fractures and activating existing ones. A major risk of this process is a possible occurrence of seismic events that can potentially be felt on the surface or even cause minor damage. In this paper, an advanced fluid injection scheme is proposed that aims to mitigate these unwanted events and to improve the permeability enhancement process. Amongst other procedures, it involves different types of cyclic injection and a traffic light system specifically designed for cyclic injection schemes. The concept is applied to develop a stimulation design for the Pohang enhanced geothermal system site in Korea, where it was first deployed in the field in August 2017.

Keywords: Hydraulic stimulation, Cyclic injection, Traffic light system, Induced seismicity, Risk mitigation, Enhanced geothermal systems (EGS)

Introduction

Economic production of a variety of geological resources, such as shale gas, tight oil, coal bed methane and geothermal heat using enhanced geothermal systems (EGS), relies on hydraulic stimulation treatments. These are reservoir enhancement methods where fluid is injected into a reservoir to increase its productivity by a combination of developing new tensile and shear fractures, and tensile opening and shearing of pre-existing fractures. Stimulated fractures may stay open naturally through the self-propping effect or they have to be kept open artificially by proppants, such as sands or ceramics that are injected together with the stimulation fluid to achieve a permanent productivity enhancement. Details about hydraulic fracturing and other reservoir stimulation methods can be found in an abundance of textbooks and other publications (e.g., Bungler et al. 2013; Economides and Nolte 2000; Economides and Martin 2007; Huenges and Ledru 2010).

While improving the hydraulic reservoir performance, hydraulic stimulation treatments also cause fluid-injection-induced seismicity. On the one hand, induced seismicity

monitoring is widely used as a tool to map fracture development and the extent of the stimulated volume (e.g., Cipolla and Wright 2000; Majer et al. 2007; Maxwell et al. 2002). On the other hand, stronger seismic events are a potential hazard caused by fluid injection (e.g., Bao and Eaton 2016; Deichmann and Giardini 2009; Ellsworth 2013). While most of fluid-injection-induced seismic events are too small to be felt at the surface, some have been large enough or close enough to the surface to be felt (e.g., Charl  ty et al. 2007) or to cause damage to buildings (e.g., Deichmann and Giardini 2009). Large magnitude seismic events (LMEs) caused by hydraulic stimulation treatments are particularly a challenge in deep EGS because typically large amounts of fluid are injected into very deep, tight and stiff formations, which are under high in situ stresses with the aim to induce shear slip on natural fractures. Examples where fluid injection led to relatively large seismic events in the past include the Cooper Basin EGS site in Australia with a local magnitude of M_L 3.7 (Baisch et al. 2006) and the Basel EGS site in Switzerland with a local magnitude of M_L 3.4 (Deichmann and Giardini 2009). Even though EGS in deep granitic basement rocks have the potential to serve as a widespread renewable baseload energy source (Tester et al. 2006), one of the reasons why this technology is not widely applied yet is the occurrence of such felt seismic events during and after fluid injection. Therefore, understanding and reducing the magnitudes of the largest fluid injection-induced seismic events is key for the technical and economic breakthrough of this technology. That is why the cyclic soft stimulation (CSS) concept was developed as a new cyclic injection scheme and traffic light system (TLS) with focus on EGS with a potential to mitigate induced seismicity.

Several factors were speculated to increase the risk of triggering LMEs. These factors include operational parameters such as injection volume (McGarr 2014), injection rate or pore pressure (Raleigh et al. 1976; Bachmann et al. 2012). Also geological reservoir parameters such as in situ stress (McClure and Horne 2014), depth and temperature of the formation (McClure and Horne 2014), and the vicinity to large faults (Wilson et al. 2018), and their orientation and degree of development (McClure and Horne 2014) were studied. Another important parameter is the permeability, which defines if a system is 'closed' or 'open'. However, these correlations are not fully understood yet. Nevertheless, based on field observations, mine-scale experiments, laboratory experiments, numerical studies and theoretical considerations, several methods were proposed to mitigate risks of induced seismicity during fluid injection. These risk mitigation measures include:

- (1) *Selection of sites with low seismic risk* Based on extensive exploration and risk assessment, a site should be chosen where the risk of inducing LMEs is low. Areas with low seismic risk are characterized, for example, by attenuating layers that damp the seismic waves on their way to the earth's surface and no active fault zones in the current in situ stress field. It has to be kept in mind that often it is very difficult to identify active faults beforehand. One example for an EGS, which has a low seismic risk due to the above characteristics, is the Gro   Sch  nebeck site in Germany (Kwiatek et al. 2010).
- (2) *Multi-stage stimulation* Especially in EGS, in the past, large net amounts of fluid (thousands of m^3) were injected in the same part of the reservoir to develop large fractures or fractured areas that act as artificial subsurface heat exchangers. If

the same amount of fluid is injected in separate parts of the reservoir via multiple stages, it is proposed that the risk of inducing larger seismic events can also be reduced (Meier et al. 2015; Zimmermann et al. 2015). Multi-stage injection was not yet extensively applied in the field for geothermal developments, but is common practice in commercial shale gas operations (Johri and Zoback 2013). One of the first field tests for EGS application is anticipated in Switzerland (Meier et al. 2015).

- (3) *Traffic light systems* TLSs are procedures where the fluid injection scheme is adapted by flow rate or pressure reduction, shut-in or flow back after predefined thresholds of seismic magnitudes, peak ground velocities or other observations are exceeded. TLS became standard risk mitigation procedures for hydraulic stimulation treatments (Bommer et al. 2015). Many TLSs were proposed (e.g., Bachmann et al. 2011; Mena et al. 2013), but only a few were tested in the field with limited success (e.g., Bommer et al. 2006; Häring et al. 2008; Kim et al. 2018a). This is due to an often observed increase in magnitudes after shut-in (Majer et al. 2007). On the other hand, TLSs are used with great success during production.
- (4) *Advanced hydraulic stimulation designs* Pressure, flow rate, fluid volume, fluid type, and injection scheme are the main parameters that can be controlled during fluid injection operations. One of the fluid injection schemes that has the potential to reduce seismicity is cyclic injection (Zang et al. 2013, 2017, 2018).

We introduce an advanced fluid injection protocol with the aim to effectively reduce the risk of inducing seismic events above a given threshold, called cyclic soft stimulation (CSS). The essence of the concept is the combination of a cyclic fluid injection scheme with a tailor-made seismic traffic light system and limited pressures, pressurization rates and injected net volumes. Special attention is given to a priori information that aid in refining the injection procedure. The concept is introduced and a site-specific cyclic fluid injection protocol and seismic traffic light system are developed explicitly for the Pohang EGS site in Korea (Lee et al. 2013; Song et al. 2015), where a first field-scale proof-of-concept experiment was performed. While a summary of the relevant results is given here, details about this field experiment can be found in Hofmann et al. (submitted).

Theoretical background

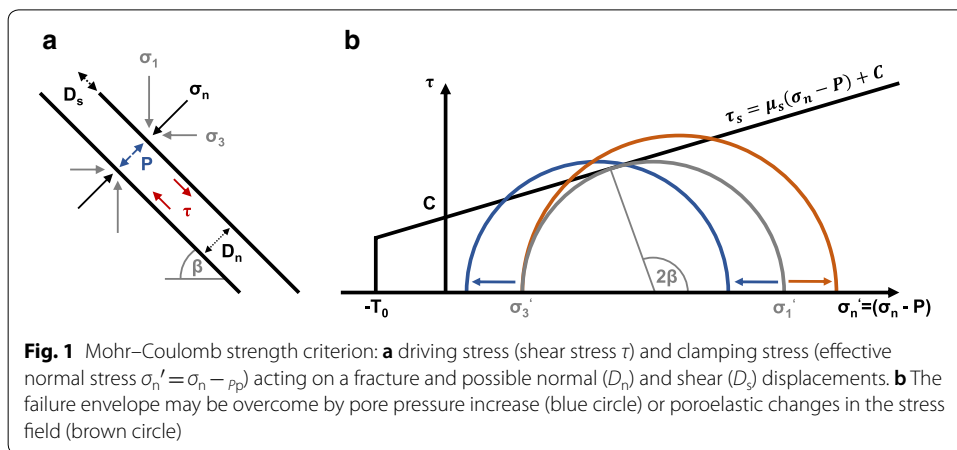
To substantiate the proposed mechanisms involved in the different components of the CSS concept, relevant geomechanical and seismological background of fluid-injection-induced seismicity and stimulation-induced hydraulic performance increase will be summarized here.

In hydraulic stimulation treatments, injection of a volume of fluid over a certain time leads to a pressure increase, which depends on the hydraulic properties of the system. The elevated fluid pressure may induce new tensile fractures (mode I failure) or trigger shear failure of pre-existing fractures or faults (mode II or III) in the rock mass. This is done to improve the hydraulic performance of the system and to increase the fracture surface area, which acts as heat exchanger area for geothermal applications. While both tensile and shear failure may occur, earthquakes result from the shear failure of pre-existing fractures or faults. Note that new tensile fractures may also shear after opening. The condition for shear failure, and hence for earthquake nucleation, is commonly

calculated by the Mohr–Coulomb failure criterion (Eq. 1), which describes the required shear stress τ to overcome the frictional shear strength τ_s of a fracture or fault depending on its cohesive strength C , the coefficient of static friction μ_s , the normal stress on the fracture or fault σ_n and the fluid pressure P .

$$\tau_s = \mu_s(\sigma_n - P) + C. \tag{1}$$

Usually, natural fractures and faults are in frictional equilibrium with the stress field in an undisturbed reservoir (Zoback 2010). Hence, fractures are stable under initial conditions and no displacement occurs when stresses and friction coefficients of faults and fractures remain unchanged. This is because the clamping stress, which is the effective normal stress acting on the fracture surface times friction coefficient, is larger than the driving stress, which is the shear stress acting on the fracture faces. Normal and shear stresses on a fracture or fault depend on fault orientation and in situ stress. Stresses and pore pressure depend on the initial pore pressure, injection rates, injection volumes, hydraulic reservoir and fracture/fault properties and time. All parameters are interacting in a complex way during stimulation and also depend on previously developed fractures. The condition for shear failure of a critically oriented fracture or fault is met once the Mohr-Circle hits the failure envelope in a naturally fractured system (Fig. 1). This slip event may lead to an improved permeability of the fracture or fault patch that slipped due to self-propping. At the same time, it radiates seismic energy. To reach this condition, the Mohr-Circle can be moved along the effective normal stress axis due to fluid pressure increase and the Mohr-Circle can be enlarged by a change of stresses. Thus, seismic and aseismic slip may be induced as a direct (fluid pressure increase) or indirect (poroelastic stress transfer) result of fluid injection due to increased pore fluid pressure, increased shear stress, or reduced normal stress on a fracture surface (Fig. 1). Therefore, the components required to cause fluid-injection-induced or -triggered seismicity are the presence of fractures or faults, fracture/fault properties (μ_s and C), fracture/fault orientations, stress magnitudes and orientations (σ_n and τ), hydraulic reservoir properties (permeability k and compressibility c), injection rates, injection volumes, and time (pore fluid pressure P). Note that seismicity may also be triggered on a ‘new’ tensile fracture after it was developed. In that regard, one may distinguish between induced and triggered seismicity. According to Cesca et al. (2013), an induced earthquake is entirely



controlled by its causative origin (e.g., pressure disturbance due to fluid injection) and would not have occurred without it. For a triggered earthquake, only the nucleation process of a small region of the rupture area is influenced by the fluid injection while the entire rupture is controlled by the background stress. Triggered seismic events are thus anticipated in view of the background seismicity rate (Cesca et al. 2013). These earthquakes are accelerated by fluid injection, but would also have occurred without it (Cornet 2012). However, discrimination between induced and triggered earthquakes is a challenging task.

The size of such a shear event may be described by the scalar seismic moment M_0 (Eq. 2; e.g., Scholz Schulz 1998) and the seismic moment magnitude M_w (Eq. 3; Hanks and Kanamori 1979; Bormann and Di Giacomo 2011). It depends on the shear modulus of the rock G , the average shear displacement on a fracture or fault during rupture D_s (slip) and the area A of the fracture or fault that ruptures during the earthquake. Another parameter in relation to the size of an earthquake is the coseismic shear stress drop $\Delta\tau$, which may be related to seismic moment and the rupture radius r_r by Eq. 4 for a circular rupture plane (Lay and Wallace 1995). LMEs occur if large parts (high A) of stiff faults (high G) slide in an unstable manner (high D_s), which is accompanied with a large stress drop (high $\Delta\tau$). Therefore, one or more of those parameters need to be minimized to reduce the seismic hazard. However, since a larger magnitude implies a larger area, large fluid-injection-induced seismic events can only occur when sufficiently large critically oriented faults with fault-rock properties facilitating brittle failure are present close to the point of fluid injection.

$$M_0 = GD_sA, \quad (2)$$

$$M_w = \frac{2}{3}(\log M_0 - 9.1), \quad (3)$$

$$\Delta\tau = \frac{7M_0}{16r_r^3}. \quad (4)$$

Statistically, earthquake magnitudes follow the equation below according to Gutenberg and Richter (1944):

$$\log(N) = a - bM_w, \quad (5)$$

where a and b are constants and N is the number of earthquakes with magnitude greater than or equal to M_w . Larger b -values are indicative for more small earthquakes and less large ones. Therefore, also the b -value should be increased to reduce the seismic hazard.

From an energy point of view, the energy supplied by hydraulic stimulation (product of fluid injection pressure and injection rate) is dissipated in a range of deformation processes (Goodfellow et al. 2015), such as formation and frictional sliding of new and pre-existing fractures, that can result in elastic wave propagation (radiated seismic energy), or occur aseismically (Cornet 2016). The ratio of energy radiated through seismic waves in relation to the hydraulic energy of the system is referred to as seismic efficiency, which is reported from a number of hydraulic fracturing operations (Maxwell 2013; Yoon et al. 2015; Goodfellow et al. 2015). Seismic injection efficiency provides an estimate of the

deformation rate in the stimulated reservoir and the efficiency of hydraulic stimulation operations (Maxwell et al. 2008). Seismic efficiency thus also serves as a qualitative estimate of seismic hazard. Low values of seismic injection efficiency are reported for hydraulic fracturing, and high values of seismic injection efficiency are attributed to stimulations that activate pre-existing faults (Maxwell 2013). Maxwell (2013) reports seismic injection efficiencies varying over many orders of magnitude from below 0.000001% to more than 1%.

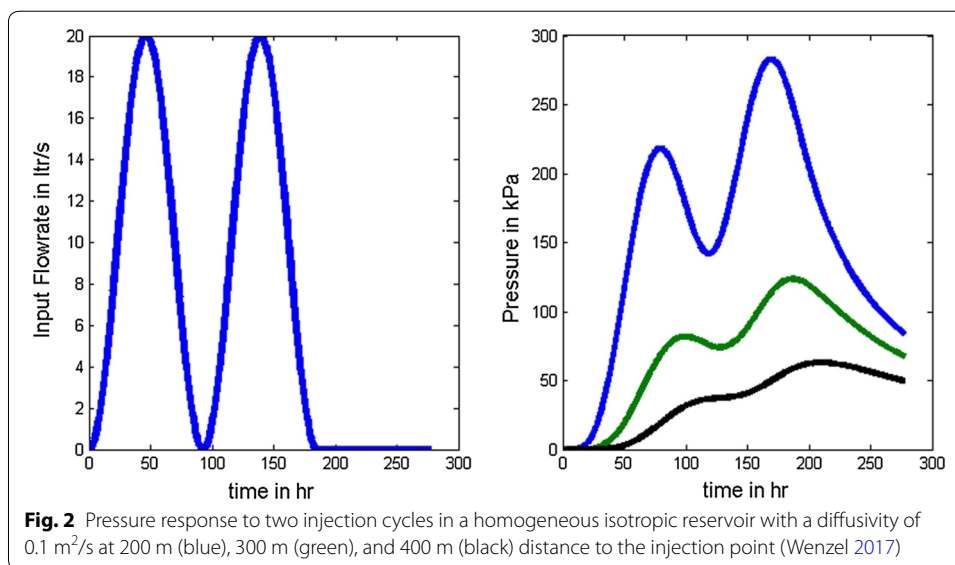
Fluid flow in a porous medium can be described by pressure diffusion, which is an extensively studied subject. The following equation provides the radial diffusivity equation with the flow term in the reservoir on the left and the material accumulation at a given point over time on the right (Economides and Martin 2007):

$$\frac{\partial^2 P}{\partial r^2} + \frac{1}{r} \frac{\partial P}{\partial r} = \frac{\phi \mu c_t}{k} \frac{\partial P}{\partial t}, \quad (6)$$

with pressure P , radial distance r , porosity ϕ , fluid viscosity μ , total compressibility c_t and permeability k . When fluid is injected during a stimulation treatment in a saturated porous rock, the speed of the resulting pore pressure disturbance is proportional to the diffusivity $\eta = \frac{k}{\phi \mu c_t}$. That means the higher the permeability and the lower the compressibility, the faster the pore pressure disturbance propagates. The storativity of a reservoir with a net thickness h can be described by the storativity $\omega = \phi c_t h$ (Economides and Martin 2007). For low-permeable basement rocks, transmissivity (kh) and storativity of fractures and faults dominate the hydraulic behavior. This is because they act as preferential flow channels with little resistance to flow and hence the equivalent diffusivity of fractured rocks can be very high. The combination of high transmissivity and small storativity in such a system can lead to significant pore pressure changes transmitted over distances of several kilometers (NRC 2013). For illustration, a calculated pressure response at 200 m, 300 m and 400 m distance to the injection point to two injection cycles is shown in Fig. 2 (Wenzel 2017).

The increased rock volume that is affected by the pore pressure change increases the risk of intersecting and activating a fault, and increases the fault surface area subject to elevated pressures. During early stage of injection, the affected volume depends on diffusivity and duration of injection, and hence on injected volume V and injection rate q ($V_a \sim V/q$), and the pressure depends on injection rate q , permeability k and time t ($P \sim q/[kt]$). During the late stage of injection, the pressure depends mainly on injected fluid volume V and storage coefficient ($P \sim V/\omega$) (NRC 2013). Davies et al. (2013) summarized the processes that may lead to a fluid pressure increase in a fault to be: (a) direct fluid injection from the wellbore into the fault, (b) fluid flow from the wellbore through stimulated hydraulic fractures into the fault, (c) fluid flow from the wellbore through pre-existing fractures to the fault, (d) fluid flow from the wellbore through permeable beds or along bedding planes to the fault, (e) poroelastic fluid pressure increase in the fault (or in fractures connected to the fault) due to deformation or “inflation” of hydraulic fractures.

The performance of a geothermal system depends on flow rates and temperatures of the produced fluid and, therefore, on the heat output. In EGS, this heat output needs to be increased since the in situ conditions are insufficient for economic production. While



the same hydraulic performance can be achieved with some highly transmissible fractures or many low transmissible fractures, the thermal performance is better in the latter case (e.g., Hofmann et al. 2014, 2016a). This is due to the increased fracture surface area that acts as heat exchanger. Often the required hydraulic performance increase is sought to be achieved by the self-propping effect resulting from shear displacement of rough fracture surfaces, which may be sufficient depending on the rock type, stress conditions and number of connected fractures (e.g., Hofmann et al. 2016b). Alternatively, proppants can be injected to prop the fractures open (e.g., Legarth et al. 2005), even though the use of proppants has been much more common in oil and gas wells than in geothermal wells.

Understanding the relation between reservoir engineering operations and corresponding seismic response is important towards the optimization of production and mitigating seismic hazard. The reduction of the total pumped volume (reduced static strain) or slow injection operations (reduced hydraulic energy rates) may reduce seismic hazard, as originally postulated in Raleigh et al. (1976) after the Rangely Colorado earthquake sequence. However, how injection parameters (e.g., pumped volume, flow rate, injection pressure) relate to seismic energy release, and in particular, to the occurrence of larger seismic events is still a matter of debate (Maxwell et al. 2015). As of today, there is no approved strategy on how to mitigate induced seismicity. Current approaches mostly focus on reactive traffic-light systems (Bommer et al. 2006) or modified hydraulic fracturing concepts (Zang et al. 2013; Meier et al. 2015).

In summary, it is necessary to reduce A , D_s , G and $\Delta\tau$ of individual shear slip events to reduce the moment magnitude of individual seismic events. Additionally, it is desired to increase the b -value of fluid-injection-induced seismic catalogs and to reduce the seismic injection efficiency to reduce the seismic hazard. At the same time, the hydraulic impedance of the stimulated system needs to be minimized and the total fracture surface area needs to be maximized. This may be achieved by developing complex fracture networks, consisting of multiple undulating and branching fractures with rough fracture

surfaces. While it is clear that this is a very challenging task, and there may be geological conditions where the stimulation design may have an insignificant effect on injection-induced seismic risk, we will explain in the following section how the cyclic soft stimulation concept is intended as one step towards a safer exploitation of unconventional geological resources by an improved seismicity control compared to massive hydraulic stimulation treatments with continuous fluid injection at constant or stepwise increasing flow rate, high pressures and large volumes.

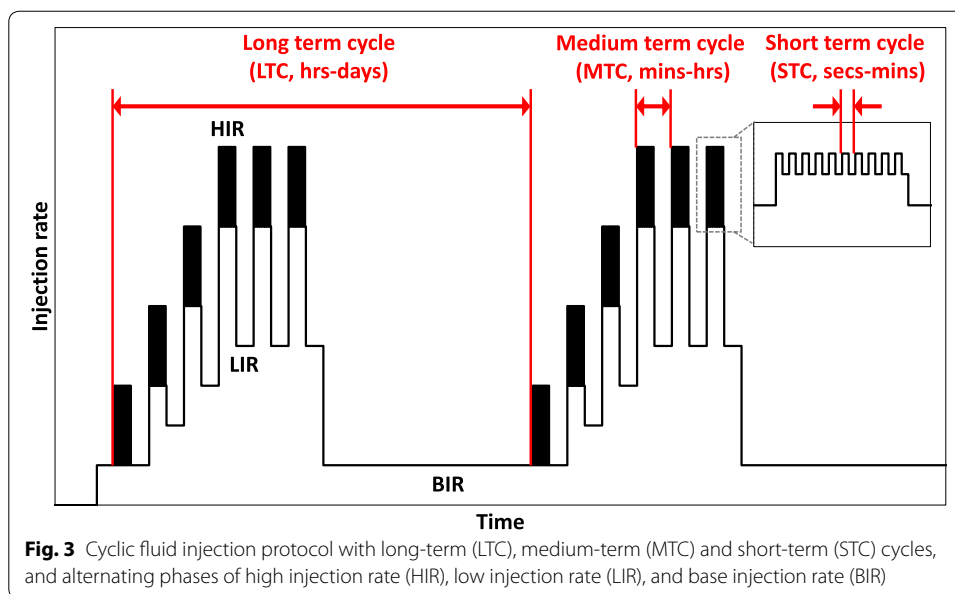
Cyclic soft stimulation (CSS) concept

One of the first cyclic hydraulic fracturing concepts was described by Kiel (1977) with the aim of improving the hydraulic properties of the stimulated rock mass. The idea of using fatigue hydraulic fracturing (FHF) procedures to reduce seismicity was introduced by Zang et al. (2013) and has later been refined (Zang et al. 2018). In recent years, experimental work at different scales revealed first insights about the influence of cyclic injection procedures on hydraulic fracture development in terms of breakdown pressure, fracture patterns, number and magnitudes of induced seismic events, permeability enhancement, and the underlying mechanisms (Hofmann et al. 2018; Zang et al. 2018). The results at different scales motivated the development of the cyclic soft stimulation concept for field-scale application and to apply it to an EGS. CSS is meant to approach two conflicting objectives: (1) minimizing fluid-injection-induced seismic hazard and (2) maximizing the hydraulic and thermal performance increase of EGS resulting from hydraulic stimulation treatments.

Besides structural geological investigations and stress field determination, before the treatment, hydraulic tests need to be performed to estimate the initial conditions and to determine the required parameters needed for the CSS concept. These tests typically include production/injection tests, extended leak-off tests, step-rate tests and one long-term CSS cycle. Afterwards, operations should be halted for some time (at least the duration of one long-term CSS cycle) to observe any delayed seismic response to these tests and to interpret the acquired data. During a treatment, the hydraulic data (flow rates and pressures) and seismicity (magnitudes, locations, focal mechanisms) are analyzed in near real time and the injection schedule is adjusted accordingly. After the treatment, additional production or injection tests should be performed to evaluate the stimulation effect.

Despite the perception that in hydraulic stimulation treatments only limited operation parameters can change the result of the stimulation (fluid type, volume, flow rate, proppants, pressure), this cyclic injection protocol offers more parameters that can be further optimized for each site for safety (to avoid large seismic events), for efficiency (to increase injectivity and productivity with reduced effort), and for data interpretability (to gain knowledge about the reservoir). At the same time the injection scheme is straightforward to execute.

We define an injection cycle as the sum of the period of high-rate injection (HIR) and the period of low-rate injection (LIR) or base-rate injection (BIR). The proposed injection protocol consists of three types of cycles with different time scales (Fig. 3): long-term cycles (LTCs, hours and more), medium-term cycles (MTCs, minutes to hours), and short-term cycles (STCs, minutes and less).



The CSS concept consists of nine major components: (1) long-term cycles (LTCs), (2) medium-term cycles (MTCs), (3) short-term cycles (STCs), (4) slow and stepwise pressure changes, (5) low pressures, (6) no shut-in, (7) limited volume, (8) traffic light system for cyclic injection, and (9) re-injection or multi-stage injection. The details of each of the components are described in the following paragraphs.

Long-term cycles (LTCs)

Long-term cycles describe the long-term (> hours) alternation between HIR and BIR in the CSS concept. The HIR phase is equivalent to the stimulation phase with fracture network opening and extension, while the BIR phase leads to pressure reduction and fracture closure. LTCs are repeated until the stimulation target is achieved or the traffic light system forces a change in injection schedule.

Injection-induced seismicity does not necessarily occur immediately at the time of injection. Instead, a delay between fluid injection and seismicity is often observed (e.g., Vlcek et al. 2017). This can occur even when a well directly intersects a fault (Davies et al. 2013). Delays can be in the order of minutes for induced seismicity on pre-existing fractures and faults, and in the range of hours and days for triggered seismicity on faults (Opsal and Eisner 2014; Vlcek et al. 2017). To name some examples, delays of ~10 h were observed between end of injection and each of the two felt seismic events at the Preese Hall shale gas development site in the UK (Clarke et al. 2014); delays from 9 min up to ~23.5 h (average ~5.5 h) were reported between the start of hydraulic fracturing treatments and induced seismic events associated with fault movements in the Horn River Basin in Canada (BC Oil and Gas Commission 2012); the delay between pressure reduction and the largest seismic event of M_L 3.4 at the Basel EGS site in Switzerland was ~12.5 h; and between shut-in and this event the delay was ~5 h (Bachmann et al. 2011). Even though seismicity at the EGS site in Basel decayed during flowback, three additional earthquakes with $M_L > 3$ occurred within 2 months after injection and

sporadic seismicity was still detected in the stimulated rock volume more than 3 years later (Bachmann et al. 2011). The reason for this time delay can be attributed to fluid storage and transmissivity of the fault in which fluid is injected (Guglielmi et al. 2008; Davies et al. 2013), to the time required for pressure diffusion through the rock mass, or to poroelastic effects that increase the fluid pressure in the activated fault (Davies et al. 2013). Hence, this time delay depends on injection parameters, and hydraulic reservoir and fault properties, as described in the previous section. Downie et al. (2010) highlights that this extended seismic activity, taking place with a delay to fluid injection, occurs primarily along faults. They report that the frequency–magnitude histogram can show b -values of ~ 2 for the fracturing phase and b -values of ~ 1 for the post-fracturing phase. Eaton and Maghsoudi (2015) also conclude that typical b -values for active faults range between 0.75 and 1.25, while during hydraulic fracturing treatments significantly higher b -values ~ 2 are observed. At mine-scale hydraulic fracturing experiments at the Äspö HRL reported by Zang et al. (2017), even higher b -values ~ 2.9 were observed (Kwiatek et al. 2018). LTCs primarily intend to include the possibility of the potentially larger, post-treatment events on faults in the treatment design. During base-rate injection, the rock mass is given time to respond seismically and stresses can relax before the start of the next cycle. The relaxation process can be described by pressure diffusion (Shapiro and Dinske 2009) and an accompanying relief in pressure, stresses and seismic energy. One LTC already leads to a certain seismic energy release due to a certain slip (D_s) of a certain area (A) of the fault. We postulate that the following pressure increase would potentially result in a smaller maximum possible seismic energy release as some of the stored strain energy in the rock mass is already released by previous events and due to a smaller maximum possible slip and fault slip area. This effect is only applicable for arrested slip events, which are the majority of the past injection-induced earthquakes according to Galis et al. (2017). However, the effect may be very small and accumulation of slip may still lead to uncontrolled ruptures. In that regard, LTCs make use of the ‘Kaiser effect’ (Kaiser 1950) that may be described in the framework of hydraulic reservoir stimulation as the absence of seismicity in a previously stimulated rock volume until the pressure level of previous stimulations is exceeded in this volume (Baisch and Harjes 2003). This effect may lead to clustering of post-injection seismicity around the outer boundary of the stimulated zone as, for example, observed at Couper Basin and Soultz (Häring et al. 2008). Additionally, the BIR phase gives the operator time to react. If injection would continue monotonically, and would suddenly be stopped after the occurrence of a LME, the delay in seismic response due to pressure diffusion would result in an increased likelihood of occurrence of larger magnitude post-treatment events. Through LTCs, the pressure would already have been significantly reduced. Therefore, the risk of inducing larger post-treatment seismic events would be smaller. In that sense, the reduced base flow rate intends to reduce the magnitude of seismic event by proactive pressure reduction and fracture closure, and allowing seismicity on faults to decay before a significant amount of additional fluid (i.e., hydraulic energy) is injected into the system.

The time delay between injection activities and seismicity may in principal be estimated if the required reservoir properties were known. Since this knowledge is usually missing, it is recommended to base the LTC length on hydraulic and seismic data from

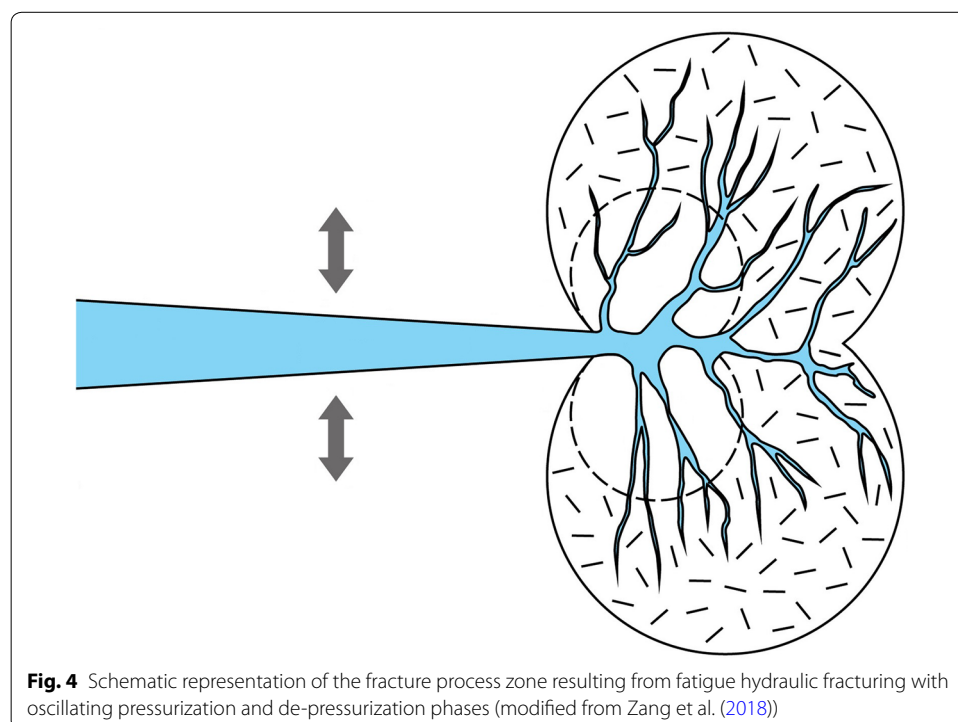
previous stimulations, if available. A simple first-order approximation method would be to determine the time delay between increase in injected volume and increase in number of seismic events or seismic moment. Cross-correlation methods may be used to get a more accurate determination of the injection-seismicity delay in these often complex datasets (Opsal and Eisner 2014). Based on this information, the duration of the BIR phase of long-term cycles should equal the time delay between fluid injection and seismicity. If no previous data from a well or a region are available, small pre-treatment injection tests are needed including at least one LTC to derive the required data before the main stimulation treatment is performed. As more data become available, these parameters should be adapted during the treatment.

Medium-term cycles (MTCs)

Cyclic injection with cycle lengths in the order of minutes to hours are called medium-term cycles in the CSS concept and comprise the HIR phase of a LTC. Different from LTCs, pressures are meant to be above the fracture opening and closure pressure throughout both, HIR phases and LIR phases, and fracture closure is avoided.

Similar to LTCs, one aim of MTCs is to incorporate the delay between fluid injection and induced seismicity (Vlcek et al. 2017) in the treatment design. The difference being that MTCs aim at the relatively short delay between injection and induced seismic events while the LTCs aim at the relatively long delay between fluid injection and triggered seismicity. An example for these relatively short delays between injection and seismicity includes the aforementioned hydraulic fracturing treatments in the Horne River Basin in Canada with delays of sometimes only 9 min between start of injection and the first seismic event associated with this injection (BC Oil and Gas Commission 2012). However, MTCs serve several other purposes as well, which are based on observations in laboratory- and mine-scale hydraulic fracturing experiments, and some field examples where cyclic injection was compared to continuous injection. Laboratory experiments performed on different intact rock and cement samples of different sizes under different stress conditions all indicate a systematic reduction in breakdown pressure (Zhuang et al. 2016, 2017, 2018; Diaz et al. 2018a, b; Patel et al. 2016; Tiancheng et al. 2018) by up to ~24% (Zhuang et al. 2016). In mine-scale experiments performed by Zang et al. (2017) at the Äspö HRL, the breakdown pressure of the progressive cyclic injection experiment was also lower (9.2 MPa) compared to two continuous injection experiments (13.1 MPa and 10.9 MPa). Two minor field-scale implications of this lower breakdown pressure are that lower treatment pressures increase the safety of the operation and reduce the pump power requirements. Mainly, the lower pressures lead to a reduced probability of occurrence of seismic events as less fractures become critically stressed (see Fig. 1). For example, in the Horne River Basin in Canada, magnitudes of seismic events show some correlation to breakdown pressure, especially near an active fault zone (BC Oil and Gas Commission 2012). Whether or not fracture re-opening or extension pressures are affected by cyclic injection remains to be investigated. At the same time, these laboratory and mine-scale hydraulic fracturing experiments show a reduction of amplitude of the largest seismic event induced by cyclic injection compared to continuous injection by ~10% to ~30% (Zhuang et al. 2017, 2018; Diaz et al. 2018a, b). Additionally, cyclic injection into the same injection interval leads to the development of

more complex fracture patterns consisting of more, but shorter and thinner, individual fractures with many branch fractures and more frequent fractures along grain boundaries compared to intragranular cracks (Zhuang et al. 2016, 2017, 2018; Zhou et al. 2017). Patel et al. (2016) found in hydraulic fracturing experiments on sandstone that the damage zone around the hydraulic fracture increased by a factor of two for the cyclic injection test compared to the monotonic injection test. Since cyclic injection tends to develop shorter fractures, an intersection with nearby faults becomes less likely, which in turn slightly reduces the potential seismic hazard. Though, the more complex fracture network potentially leads to an increased hydraulic and thermal performance. While the influence of cyclic injection on the hydraulic performance of the system is unclear from these experiments, as it is sometimes better (e.g., Patel et al. 2016) and sometimes worse (e.g., Zhuang et al. 2017, 2018), field evidence suggests that the increased complexity of fracture growth leads to larger stimulated reservoir volumes, larger fracture areas, and a better connectivity between the stimulated fractures and intersecting natural fractures (Kiel 1977; Inamdar et al. 2010). This is proposed as one potential reason for increased production from multi-stage hydrocarbon wells subject to cyclic injection compared to the ones treated with monotonic injection schemes. The effects described above are potentially related to enhanced microcrack development and subcritical crack growth. Figure 4 schematically illustrates how cyclic pressurization shall stimulate the rock mass at a distance to the injection well. Zang et al. (2018) showed that the injection efficiency (ratio of radiated seismic energy to injected hydraulic energy) decreases with increasing number of cycles in laboratory and mine-scale cyclic injection experiments compared to continuous injection. The reason for this observation remains to be clarified. In addition to the above, cyclic injection data can be used for hydraulic reservoir characterization in



the frequency domain (Fokker et al. 2017 and references therein). This analysis can best be done for the MTCs since LTCs do not have constant flow rates and for short-term cycles (STCs) the area of investigation is too small and data quality is often poor. The advantage of this method is that the hydraulic reservoir properties can be determined dynamically during injection.

The length of MTCs depends on the number of cycles required for the initial progressive cyclic injection phase (depending on the data available from previous injections, a minimum of four to six cycles are required to determine the fracture opening pressure FOP based on a change in slope in the pressure–flow rate curve, with two or three data points below the FOP in the matrix flow-dominated regime and two or three data points above the FOP in the fracture flow-dominated regime) and the uniform cyclic injection phase (according to Fokker et al. (2017), a minimum of five cycles is required for good data quality of hydraulic pulse testing analysis, if this analysis is intended to be done), and the length of the LTCs. The optimization of this and other parameters needs to be further researched. Since cyclic opening and closure of fractures may damage the fracture transmissivity (e.g., Vogler et al. 2016), the pressure of the uniform cyclic injection phase should not be below the fracture closure pressure. Maximum pressures are discussed below. Flow rates should be chosen accordingly.

Short-term cycles (STCs)

STCs, with cycle lengths in the order of minutes or less, may be added on top of the MTC HIR phases. Due to the short cycle length, STCs can also be referred to as pressure pulses.

Similar to MTCs, in STCs uniform cyclic injection intends to reduce the maximum magnitude of induced seismic events, to reduce the fracture breakdown pressure, and to increase fracture network complexity. The shorter pressure pulses are intended to amplify the fatiguing and weakening of the rock by inducing additional small fissures before and besides macroscopic fracture development. In reported experiments, often these cyclic injection effects were increased when more cycles were performed (e.g., Zang et al. 2018). For example, Diaz et al. (2018a, b) observed a decrease in maximum acoustic emission amplitude, fraction of tensile cracks (compared to shear cracks) and seismic injection efficiency with increasing number of cycles and Zhuang et al. (2016) reported development of multiple branching fractures specifically for high cycle numbers. Additionally, they pointed out that such a complex fracture pattern was also observed for a case where 150 cycles were performed without failure followed by monotonic injection until failure. This experiment suggests that small fissures are induced by cyclic injection before macroscopic failure. These large cycle numbers can only be achieved by very short cycle lengths, which results in STCs. Since the “hydraulic fatigue” effect is the main purpose of STCs, more details about fatigue are given here. While experiments and theories about hydraulic fatigue of rock are limited (e.g., Zang et al. 2018; Hofmann et al. 2018), a much larger number of experiments and theories exist that investigate and describe “mechanical fatigue” of rock without fluid injection (e.g., Cerfontaine and Collin 2017) and mechanical fatigue of industrial materials by cyclic loading (e.g. Fatemi and Yang 1998). Mechanical and hydraulic fatigue behavior relies on the heterogeneity and imperfections of the medium that is subject to load or pressure cycles.

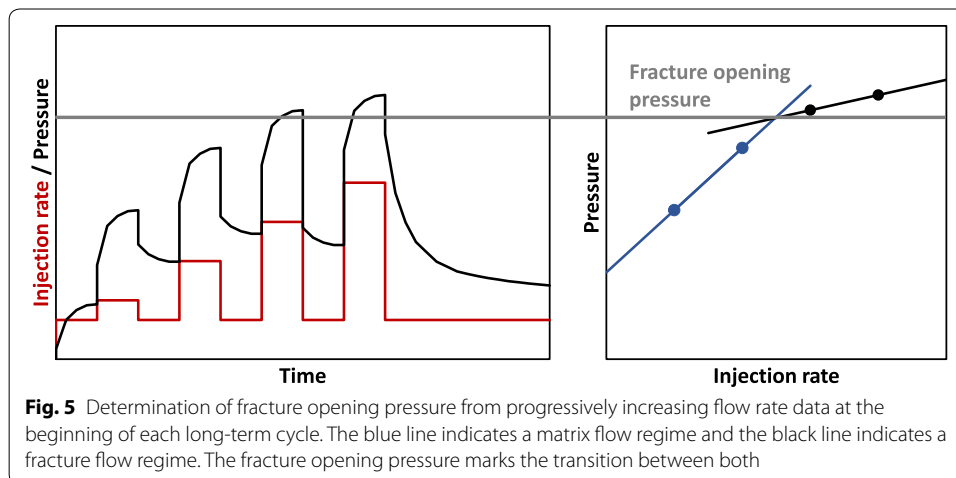
Since rock masses in general are very heterogeneous and intersected by faults, fractures and fissures at all scales, fatigue behavior is likely more pronounced in geological media compared to engineered materials. Whether and how classical fatigue concepts can be applied to hydraulic fatigue by cyclic injection and pressure pulses remains subject of further research. Observations from cyclic loading experiments on rock, for example, show that besides the strength reduction, additionally, cyclic loading has the potential to decrease Young's modulus (up to ~33%) and increase Poisson's ratio (up to ~600%) with increasing cycle number (Heap and Faulkner 2008; Heap et al. 2009, 2010; Cerfontaine and Collin 2017). Thus, Shear Modulus G of the tested specimens is reduced, which would in turn potentially result in a magnitude reduction of induced seismic events (cf. Eqs. 2, 3). In the cyclic loading experiments by Heap et al. (2009, 2010), summarized by Cerfontaine and Collin (2017), G is reduced by ~43% from ~13.5 to ~7.7 GPa after 14 cycles. However, these mechanical cyclic loading experiments were conducted over a large stress range (from 0 to >100 MPa). In cyclic injection, the effective stress changes are usually much lower. Therefore, reduction of G can only be seen as a minor possible result of cyclic injection which remains to be proven, but not as its main purpose. Other rock properties are also affected by mechanical cyclic loading. For example, Erarslan et al. (2014) found that tensile cyclic loading of Brisbane tuff led to a reduction of static fracture toughness by up to 46% and a reduction of indirect tensile strength by up to 36%. G , fracture toughness and tensile strength reduction are also interpreted to be a result of microcrack development in the rock matrix. Ghamgosar and Erarslan (2016) illustrate the complex and wide fracture process zone resulting from cyclic loading of Cracked Chevron Notched Brazilian Disc Cadia Valley monsonite and Brisbane tuff specimens using computer tomography scans. Stephansson et al. (2018) performed cyclic injection tests with pressure pulses on top of progressively increasing pressure cycles at laboratory scale and found a breakdown pressure reduction from ~10 to ~20% for fine-grained granite and diorite-gabbro, but no effect on Ävrö granodiorite, which suggests that hydraulic fatigue behavior is material dependent. A major motivation to apply STCs is that, compared to MTCs, in the mine-scale experiments performed by Zang et al. (2017), additional pressure pulses led to the largest hydraulic performance increase of all tested injection schemes (Zimmermann et al. 2018). More details about the hydraulic fatigue concept can be found in Zang et al. (2013, 2017, 2018).

When choosing the HIR and LIR flow rates for STCs, one has to keep in mind that, due to the short time of the pressure fluctuations, the maximum pressure recorded in the well will be similar to the maximum pressure resulting from constant injection with an average rate of HIR and LIR. The difference between HIR and LIR, and the frequency of the pressure pulses is subject of future optimization studies to minimize seismicity and maximize hydraulic performance increase. Depending on the purpose, the LIR injection rate may be chosen to always have the same difference between the HIR and the LIR in all MTCs to make them comparable for harmonic pulse testing analysis, to be equal to about half of the HIR, to stay above the fracture opening pressure to avoid fracture damage, or to be equal to the BIR to increase the effect of pulsed injection.

Slow and stepwise pressure changes

Each LTC starts with MTCs of progressively increasing injection rates with the same cycle length before the following cycles are repeated with the same flow rates. Hence, the CSS concept consists of a combination of progressive cyclic injection in the beginning followed by uniform cyclic injection and ending with a LIR phase before the BIR phase.

One reason for the progressive cyclic phase is to determine the fracture opening pressure (FOP) by identifying a distinct change in the slope of the pressure–rate curve (Fig. 5). This pressure is the point when matrix-dominated flow shifts towards fracture-dominated flow and is an indication for the development of a new hydraulic fracture or opening/propagation of an existing fracture. Low pressurization and depressurization rates intend to lower the slip on faults caused by fluid injection, which in turn lowers the magnitude of triggered seismic events. Evidence for this process was found, for example, by French et al. (2016), who observed less slip and a lower shear stress drop in laboratory experiments on Sandstones when using a slow pressurization rate compared to fast pressure changes. Besides this effect, slower pressure changes likely increase the *b*-value of induced seismicity in intact rock as well. This was, for example, observed in rock mechanics and structural mechanics testing, where slower mechanical loading rates led to an increased *b*-value (e.g., Sagar and Rao 2014). Additionally, pressurization and de-pressurization rates seem to influence the fracture pattern, which tends to be more complex with smaller individual fractures for lower loading rates (e.g., Lahaie and Grasso 1999). Wang et al. (2018) found that the peak strength of a sample is reduced when subject to lower mechanical loading rates. Sano et al. (1981) showed in unconfined compression experiments that low strain rates reduce the strength of a specimen. In addition, Sano et al. (1982) found that the *b*-value is increased when the strain rate is reduced. Thus, this progressively increasing stepwise flow rate increase is meant to ensure a slow pressure increase, which is interpreted as slow loading rate or strain rate. In addition, the last LIR phase before the BIR phase is used to avoid abrupt pressure reduction and fracture closure (Fig. 3). The flow rate of the LIR phases of these MTCs should also be chosen to avoid abrupt pressure reduction and fracture closure during the stimulation phase. As



stated earlier, the reason for keeping the fracture open is that frequent fracture opening and closure may result in permeability reduction due to fracture surface degradation and gouge formation by asperity destruction (Vogler et al. 2016).

During the initial progressive cyclic injection phase, the pressure steps should be of equal size and cycle lengths should also be equal. Rates may be chosen that at least two (better three) steps with increasing flow rates can be accommodated before, and another two (better three) steps with increasing flow rates after fracture opening occurs to be able to identify the FOP. Multiple uniform pressure cycles may follow depending on the anticipated LTC length and maximum pressure. The cycle length should, in the best case, be long enough to reach quasi-static bottomhole pressures. That means, in low-permeable formations (<5 mD) each injection phase should last for at least 1 h. Constant rates and equal time steps are critical for accurate test analysis. For improved analysis, bottomhole pressure gauges may be used. Alternatively, bottomhole pressures may be calculated from wellhead pressures and frictional pressure loss calculations.

Low pressures

Once the pressure during the progressively increasing flow rate steps at the start of each LTC is above the FOP, the same cycle is repeated until the end of the HIR phase of the LTC. This way the pressure is high enough, but not significantly higher than necessary, to stimulate the reservoir.

A direct correlation between pore pressure and seismic hazard (magnitude) is currently unknown (e.g., Bachmann et al. 2012). However, it was speculated that the b -value reduction with increasing distance from the injector is likely due to the lower pore pressures in this area and that this effect increases with distance and time (Bachmann et al. 2012). The reason for this behavior is that critically stressed faults under high shear stress only need a very limited pressure increase to fail. However, this b -value reduction is also caused by an increase in number of small seismic events close to the well due to the elevated pressures, which activate also less favorably oriented fractures with lower shear stress resolved on the fracture surfaces. Certainly, applying lower pressures will not increase the magnitude of a seismic event caused by fluid injection because when larger pressures would be applied, the event caused by lower pressures would happen anyway, potentially even earlier. Galis et al. (2017) suggest that it depends on the magnitude of a pore pressure perturbation and the affected area if a fault rupture is arrested (subcritical) or runaway rupture of the whole fault is triggered (supercritical). We propose that the application of low-pressure injection lowers the seismic hazard because of the following reasons. First, lower pressures require lower injection rates. This implies a smaller volume injected over a fixed period of time. If a critical seismic event occurs, the corresponding reaction (e.g., flowback) from the traffic light system would be more efficient as critical faults are approached more slowly by the pressure front. Second, the volume of influence which is affected by the imposed pressure change is smaller when lower pressures and flow rates are used. This reduces the likelihood of intersecting critically stressed fractures and faults, and the fault area affected by a pressure disturbance is reduced. Third, keeping the treating pressures low ensures low net pressure in the fracture system which in turn minimizes fracture opening, and the resulting poroelastic

displacement and stress increase, which could potentially trigger more seismic events, are smaller. Thus, the seismic hazard is further reduced.

If the hydraulic performance is improved during the treatment and seismicity allows, the required flow rates to reach the opening pressure will increase. If the hydraulic performance is not improved, flow rates and pressures may be increased further above the FOP to improve the stimulation effect. The maximum fluid pressure should be maintained below the critical effective stress state for fault activation. This can be estimated from slip tendency analysis of nearby faults (e.g., Blöcher et al. 2018). If the confidence on in situ stress state and fault geometries is low, it is recommended to apply the lowest possible pressures that lead to a stimulation effect and to avoid excessive overpressures. This minimum necessary pressure should be determined using the data from progressively increasing flow rate cycles as explained above.

No shut-in

The CSS concept foresees no shut-in period at any time. The only exceptions are after initial injection tests before the main treatment, and long after the treatment after a new reservoir equilibrium is reached. Instead, the flow rate is reduced to a base injection rate (BIR) during the treatment and flowback may be initiated in response to seismic events that trigger the traffic light system.

Base-rate injection without shut-in has several purposes: continuous injection leads to a slower pressure reduction and also a less abrupt pressure increase during next day's HIR phases (see reasoning for slow pressure changes above). In the past, it was observed that the largest events occurred during shut-in (e.g., M_L 3.4 event in Basel a few hours after shut-in; Deichmann and Giardini 2009). The occurrence of larger magnitudes after shut-in can be explained by the pressure diffusion process, which keeps the area affected by pressure increase growing after shut-in. This leads to a continuing increase of area of fault surfaces subject to this pressure increase and an increased number of affected fractures and faults at the boundary of the pressure front will be brought further to criticality. Nevertheless, the consistent observations of large magnitude earthquakes during shut-in are counter intuitive, since the pressure diffusion process is slower during shut-in than during continuous injection. The postulation that a larger magnitude earthquake during shut-in would not have occurred if injection had continued makes this phenomenon somewhat enigmatic. Barth et al. (2013) even suggest that the probability of occurrence of a larger seismic events can be reduced for a short time by continued injection compared to an abrupt shut-in. Mukuhira et al. (2017) explain the reason for the occurrence of the largest magnitude events during shut-in by pore pressure migration at the Basel EGS site the following way. They found that during shut-in seismicity still extended outside the edge of the previously stimulated zone with the largest magnitude events occurring in this area. The reason for this was progressing pore pressure increase at the edge of the seismic cloud with pressures high enough to induce seismic events. This is because during stimulation a pressure gradient exists between the injection point and the periphery. This pressure gradient disappears because both the pressure source and the flow resistance are lost. The high pressure from the injection point migrates towards the far field leading to a pressure increase at the edge of the seismic cloud. Because of the low permeability outside of the stimulated zone, this high pore pressure stagnates in this

area. Due to preferential flow along faults, the pore pressure redistribution leads to large areas of critically stressed fractures to fail and cause LMEs. Besides, continuous injection of cold fluid also leads to a thermal stimulation (Grant et al. 2013) of the reservoir, which induces small fissures and fractures in addition to the larger scale fractures, and thus eases further fracture development and extends the stimulated subsurface fracture system which will be more complex with a larger surface area as a result. Note that the “thermal front” and the “pressure front” do not coincide. Typically, the “thermal front” is lagging far behind the “pressure front” and both do not coincide with the “fluid flow front” (tracers). Additionally, if seismic events occur at base rate, there is still room to react by flow back if unwanted large events should occur. For flow back, sufficient storage space must be available on site and fast transportation of potentially produced waste water to a water treatment facility needs to be ensured.

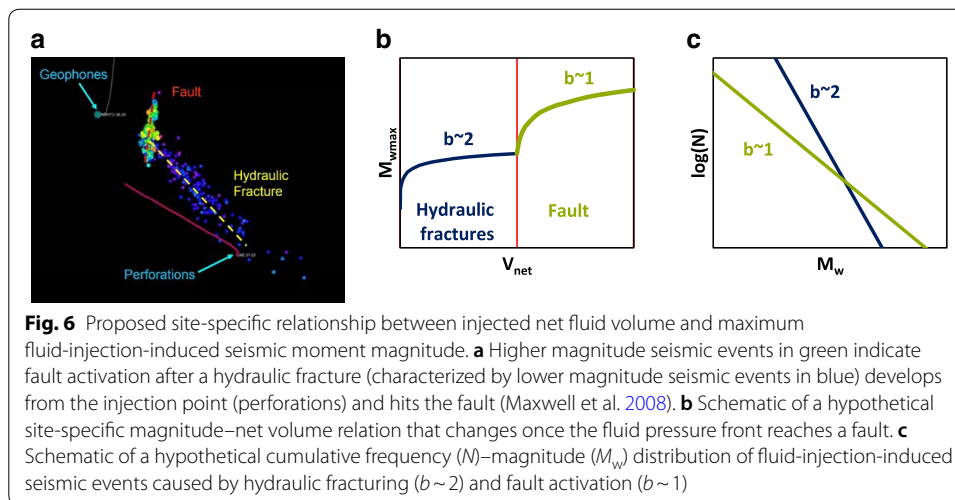
The BIR should be chosen such that the pressure is reduced below the fracture closure pressure during the BIR phase. It is limited by the minimum stable flow rate that the pumps can achieve, but may be increased if the injectivity increases. Flowback is to be initiated based on the traffic light system (see below).

Limited volume

The CSS concept includes a limitation of the maximum injected net fluid volume. This limitation is based on a site-specific net volume–magnitude relation and additionally enforced by a site-specific traffic light system.

As described earlier, magnitudes of induced seismic events during hydraulic stimulation treatments are correlated with the injected net fluid volume (McGarr 2014; Zang et al. 2014; Shapiro et al. 2007, 2010). This may not be valid anymore for long-term circulation (injection and production). Larger fluid volumes lead to a higher potential to induce larger magnitude events since a larger reservoir volume will be affected by the induced pressure increase and, therefore, it is more likely that a critically oriented fault is intersected by the pressure perturbation. We propose that site-specific magnitude–volume relations can be derived for induced seismic events not affected by fault zones. This site-specific relation needs to be established either on the basis of existing data from previous injections or on the basis of smaller injection tests before the main stimulation treatment. Resulting b -values will be ~ 2 , if seismicity is not influenced by faults. Figure 6 shows this conceptually. An example from a specific site cannot be provided here due to the lack of published data. If potentially hazardous faults are present in the vicinity of the wells (Wilson et al. 2018), this site-specific relation between magnitude and volume would change once the pressure front reaches the fault and overcomes the critical pressure for slip. Since the b -values for seismic events triggered on fault zones (tectonic events) are much lower (~ 1) compared to induced seismic events (~ 2) in undisturbed rock mass (Eaton and Maghsoudi 2015), the magnitudes would suddenly increase stronger with injected volume during a hydraulic stimulation treatment (Fig. 6).

We propose that, for hydraulic stimulation treatments, a specific magnitude–net volume relation exists for each site for a large range of injection volumes, if no large-scale faults are present in its vicinity. If a site-specific relation is confirmed, it allows to determine the maximum amount of injected fluid to stay below a given maximum target magnitude for the site. If this critical volume is identified before the treatment

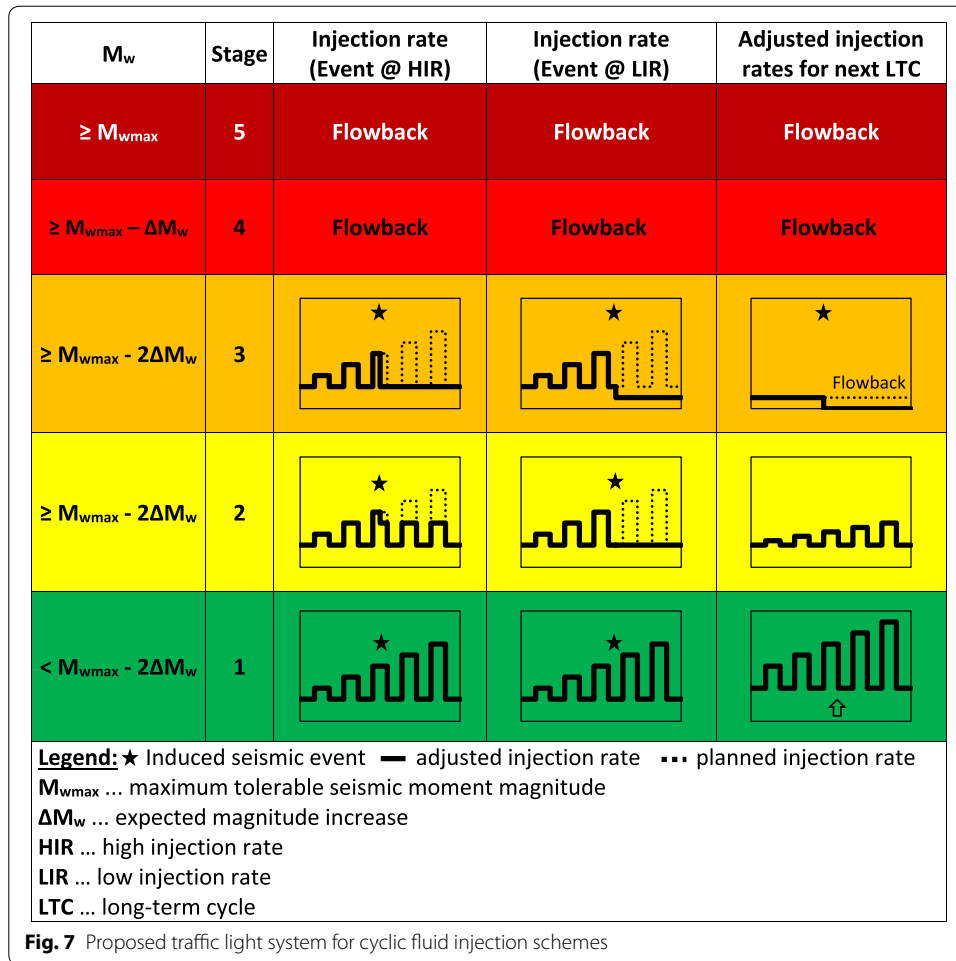


from existing data, the maximum injected volume needs to be planned accordingly. If the relation is derived from a continuing stimulation, it needs to be adjusted accordingly. If a fault is present, a deviation from this site-specific magnitude–net volume relation may be observed. Independent if this point of significant b -value change can be identified from previous treatments or from an ongoing stimulation, it marks the maximum net injection volume to avoid fault activation. Thus, by monitoring net injection volume and moment magnitudes of seismic events, critical net volumes can be used as an addition to the traffic light system presented below. For example, the well could immediately be flowed back if a sudden decrease in b -value (sudden increase in magnitude) is observed or the well should slowly be shut-in if the pre-determined maximum net volume is reached. This behavior may in theory be estimated before a treatment based on a structural geological model including the major fault zones, knowledge about stress magnitudes and directions, and the hydraulic behavior of the system. However, the heterogeneous nature of rock masses and the limited data about the subsurface would make this estimation very difficult.

Traffic light system for cyclic injection

In the described cyclic injection scheme, high-flow rate (HIR) phases are alternating with low-rate (LIR) or base-rate (BIR) phases with a very low injection rate. To avoid induced seismic events with a magnitude above a given threshold, a seismic traffic light system is needed to effectively mitigate these LMEs. In the context of cyclic stimulation, the immediate action items in the traffic light system were divided into actions during a high-injection rate phase (left column “Event @ HIR”) and actions during low- or base-rate injection (right column “Event @ LIR”). In addition to the immediate action items, the schedule for the next LTC is also adjusted based on the measured seismicity. This procedure aims to limit the injected volume to an amount that can safely be injected, with the purpose to stimulate the reservoir as much as possible.

The proposed advanced traffic light system for cyclic fluid injection schemes is shown in Fig. 7. Magnitude (or peak ground velocity) thresholds should be derived for each site



individually and is often defined by national legislation. The target of the proposed traffic light system is to mitigate the occurrence of induced seismic events with a magnitude above the threshold M_{wmax} given in Stage 5. This critical magnitude is to be determined by a risk assessment study for each site individually (Majer et al. 2012). We propose to determine the difference in magnitude between the stages ΔM_w based on the largest difference in magnitude between the largest seismic event and the next largest one. The intention is to increase the likelihood that one TLS stage is activated after another (e.g. from green to yellow) and big jumps between TLS stages (e.g. directly from green to red) are avoided. However, it can only be determined from previous stimulation data or injection tests.

The following procedures are carried out if events with the given magnitudes occur:

Stage 1—green The treatment is continuous according to schedule independent of the injection phase. For the following LTC, the injection scheme may be repeated or changed depending on the flow rates required for fracture opening. This decision is based on the hydraulic data from the previous LTC.

Stage 2—yellow If the event overcomes this threshold, the flow rate is going to be reduced depending on the injection phase at which the event occurred. If it was detected during a HIR phase, the flow rate is reduced to the level of the previous HIR phase. Subsequent HIR phases during that day are also limited to this level. If an event is detected during low-rate or base-rate injection, no further HIR phases will be performed during that LTC. For both cases, the maximum injection rate of the following LTC is limited to the maximum injection rate before the seismic event occurred.

Stage 3—orange At this threshold, the flow rate is reduced to the LIR, if the event occurs in the HIR phase. If it occurs in the LIR phase, it is reduced to the lowest possible BIR. In both cases, the flow rate is not increased again during that LTC and during the next LTC. If another Stage 3 event occurs during the lowest BIR, the well is flowed back. The flow back rate will depend on the pressure, injected volume and hydraulic properties of the system. After a full decline of the seismicity and a re-assessment of the seismic risk, the CSS treatment may commence.

Stages 4 and 5—red If the Stage 4 threshold is overcome, the pressure will be released by a complete flow back independent of the injection phase. Stage 5 is only given here as reference to the maximum allowable magnitude. Again, injection may only commence after seismicity diminished fully and the seismic risk is re-assessed.

Re-injection or multi-stage injection

At the end of the treatment, injection is continued at the base rate until the pressure is below the fracture closure pressure. Should this not lead to the required pressure reduction, the well should be flowed back. After that the well may be shut-in. We showed previously that the maximum volume that should be injected during a CSS treatment is determined based on a magnitude–volume relation and is in addition subject to a traffic light system. If possible, all of the injected fluid should be produced back after the treatment if significant seismicity levels (e.g., red traffic light alert) were reached. The earliest that the well should be shut-in is after the pressure is below the fracture closure pressure.

If a treatment did not achieve the required hydraulic performance increase at the time when this maximum injectable volume is reached, there are two alternatives to further stimulate the reservoir. The first option is to re-inject the fluid that was produced back into the same open hole area after adequate treatment. The second option is to stimulate the well in multiple stages (Majorowicz et al. 2013; Meier et al. 2015) where the same amount of fluid is injected again in the next stages.

Cyclic soft stimulation concept for the Pohang EGS well PX-1

The Pohang EGS Project

The Pohang EGS is the first geothermal electricity generation project attempted in Korea, which was initiated in 2010 (Song et al. 2015). The granodiorite and granitic gneiss were accessed by the deviated well PX-1 and the vertical well PX-2 which reached a measured depth of 4362 m and 4348 m, respectively (Kim et al. 2017). Multiple hydraulic stimulation treatments were performed at the site in 2016 and 2017 (Kim et al.

2017; 2018a; Park et al. 2017a, b, Kim et al. 2018a). The magnitudes of the largest seismic events during PX-1 and PX-2 stimulations were reported as 2.3 (Kim et al. 2017) and 3.1 (Grigoli et al. 2018), respectively. Therefore, mitigation measures were necessary at this site that limits the maximum magnitudes of induced seismic events. This was attempted by developing the CSS concept for well PX-1 based on the data from the previous stimulations at the site. The derivation of this site-specific CSS injection scheme and traffic light system is described below.

Derivation of the site-specific cyclic soft stimulation scheme and traffic light system for Pohang well PX-1

Here, the initial setup of the injection scheme and traffic light system for the Pohang cyclic soft stimulation treatment in August 2017 in well PX-1 is presented. It is based on the ideas presented above and the data from the previous stimulation treatment in December 2016 in well PX-1 (Kim et al. 2017).

The goals of the treatment were to reduce the magnitude of induced seismic events below M_w 2.0, to map the stimulated reservoir volume and to test the cyclic soft stimulation concept in the field. Secondary targets were hydraulic performance increase and hydraulic connection of the two wells.

Long-term cycles

The delay between injection and seismicity is difficult to assess without advanced cross-correlation methods because of the frequent changes in injection, shut-in and flow back phases. As a simple approximation, we identified that the delay between the start of injection and the increase in number of seismic events was about half a day for the monotonic 10 l/s injection during the December 2016 stimulation in PX-1. Additionally, the first seismic event occurred about half a day after the opening pressure was reached for the first time. Based on this, the length of the LTCs was chosen to be 1 day. To accommodate more MTCs, the HIR phase was extended to 14 h and the BIR phase was reduced to 10 h. For the ease of execution, the HIR phase was planned to start in the morning and end in the evening while the BIR phase was planned for the nighttime.

Medium-term cycles

The length of MTCs was chosen to be 2 h. This allows to perform at least four cycles for the initial stepwise pressure increase and three more repetitions of the last cycle at the maximum flow rate.

Short-term cycles

To accommodate ten STCs in each HIR phase of a MTC, which has a length of 1 h, a STC length of 6 min was necessary. This number of cycles ensures that STC data can be analyzed by hydraulic pulse testing analysis and is at the same time long enough to be operationally feasible for the pumps used in the treatment. The HIR of STCs was always 1 l/s above the equivalent rate of the MTC HIR phase while the LIR of the STCs was always 1 l/s below that rate. This way, the difference between the HIR and LIR of the STCs was the same throughout the treatment.

Slow and stepwise pressure changes

In the previous stimulation in PX-1, the fracture opening pressure was determined to be between 15 MPa and 17 MPa wellhead pressure, which indicates shearing of pre-existing fractures rather than tensile hydraulic fracturing (Park et al. 2017a, b). 17 MPa WHP was reached with an injection rate of 6 l/s within less than an hour time. At 10 l/s, the WHP was still less than 19 MPa and, therefore, only slightly above the opening pressure. Since only four pressure steps can be performed during each LTC, the flow rate was increased in steps of 2 l/s from 4 to 10 l/s. For the initial fracture opening pressure determination test, pressure steps of 1 l/s were planned to increase the resolution. During cycling, the flow rate was planned to be reduced to half the rate of the HIR to keep the fractures open when cycling between 5 and 10 l/s, and to ensure slow pressure changes.

Low pressures

Based on the step rate test results discussed above, the rates during initial injectivity determination should stay below 4 l/s to avoid fracture opening. The flow rates during stimulation phases should be between 4 l/s, which was the lower limit for fracture opening, and 10 l/s, to prevent unnecessary overpressures. The maximum injection rate should be more than 6 l/s to ensure that the fracture network is hydraulically stimulated. It could reach up to 10 l/s since the cyclic injection leads to lower pressures compared to continuous injection as no steady-state condition will be reached.

No shut-in

Shut-in is only foreseen after the initial injectivity tests. The lowest possible rate that can be achieved with the mud pumps used for the treatment is 1 l/s. Therefore, the BIR was 1 l/s with the possibility to increase it to 2 l/s if required.

Limited maximum volume

At the start of the CSS treatment, the initial net volume (V_{net}) injected in PX-1 was about 1500 m³. This is the difference between the cumulative volume that was injected into PX-1 and the cumulative flow back volume from PX-1 before the start of the CSS treatment. Events above M_w 2.0 occurred at about $V_{\text{net}} \geq 3675$ m³. According to this observation, ~2175 m³ of fluid could be injected during the CSS treatment. Subtracting a safety margin of about 175 m³, the total injected net volume of the soft stimulation treatment should, therefore, be less than ~2000 m³ to avoid injecting critical amounts of water and to keep the magnitude below the target level of 2.0. Potential fluid losses were not considered in this analysis.

Traffic light system for cyclic injection

While the injection scheme is subject to daily changes, the traffic light system has to remain unchanged during the course of the treatment. The traffic light system for the cyclic injection scheme presented above equals to the one presented in Fig. 7 including the presented action items. Here, we introduce the corresponding levels of seismic moment magnitude thresholds to be inserted in Fig. 7 leading to the site-specific traffic

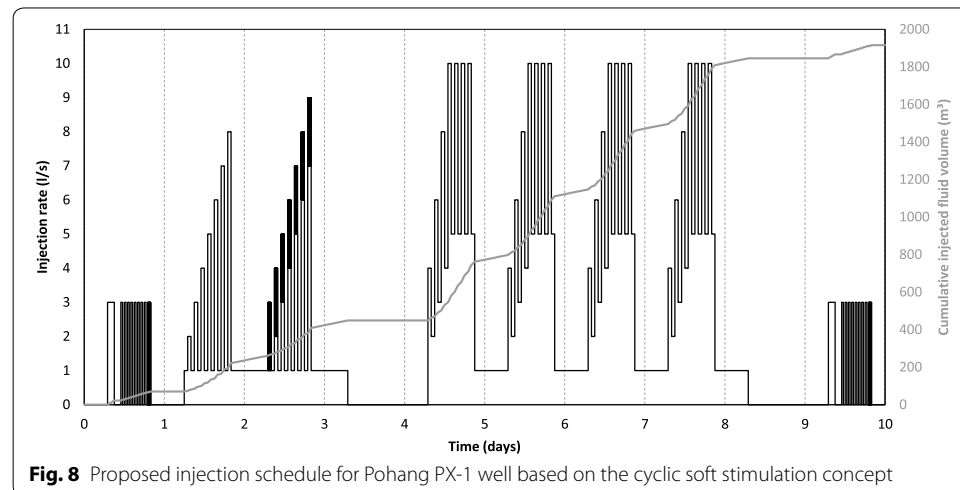
light system for the Pohang soft stimulation treatment. The critical magnitude to be avoided is M_{wmax} 2.0, which is the same as the criterion from the first stimulation (Kim et al. 2018a) and a reduction by 0.5 from the second and third hydraulic stimulations in Pohang. This is because magnitudes below 2.0 are hardly perceived by local residents and this magnitude is also the reporting criterion of the Korean Meteorological Administration (KMA) to the general public (Kim et al. 2018a). Therefore, Stage 5 is reached once a local magnitude above 2.0 is detected. Except for the initial events at magnitudes below 0.5, the difference ΔM_w between the maximum magnitude of a seismic event and the subsequent larger magnitude event was less than 0.3 in the previous hydraulic stimulation of PX-1. Therefore, the stages in the traffic light system are separated by $\Delta M_w = 0.3$. This results in threshold levels of $M_w = 1.7$ for Stage 4 and $M_w = 1.4$ for Stage 3. Since the threshold for Stage 2 was 1.0 in the traffic light system for the previous stimulations (Kim et al. 2018a), this level was adjusted from $M_w = 1.1$ to $M_w = 1.0$. Since only M_L data are available from previous stimulations, M_L and M_w are assumed to be the same for this consideration.

End of the treatment

In conjunction with the maximum injectable net volume, these flow rates and cycle durations limit the time of the total treatment to about 10 days including pre- and post-treatment tests as well as shut-in phases. After the pressure is reduced below the fracture closure pressure during the last BIR phase, the well may be shut-in. Once the pressure level reaches initial values, the same injection tests from day 1 should be repeated to evaluate the hydraulic performance change induced by the treatment. If the goals of the stimulation are not reached and further stimulation is needed this has to be done after flowing back the injected volume and re-injecting not more than that same amount.

Summary of the cyclic soft stimulation scheme for Pohang well PX-1

The complete cyclic injection scheme is described below as shown in Fig. 8. It should be adapted on a daily basis based on pressure and seismicity development.



Day 1 (injection tests)

To determine the initial injectivity, several tests were foreseen for the first day. These include a short-term injection test at a flow rate of 3 l/s for 2 h followed by 2 h of shut-in to observe the initial reservoir response. At this rate pressures are expected to stay below the opening pressure. This is necessary to determine the undisturbed initial well performance before stimulation. This test is followed by two hydraulic pulse tests. The first one with 30-min injection is followed by 30-min shut-in (eight cycles). This test is carried out to compare the pulse test with the conventional injection test. The second pulse test is conducted with ten cycles of 3-min injection and 3-min shut-in. The purpose of this second test was to have a baseline for comparison with later hydraulic pulse tests which are performed on top of medium-term cycles. During these initial injection tests, it has to be ensured that pressures do not overcome the expected opening pressure of 15–17 MPa WHP.

Day 2 (progressive cyclic injection)

The progressive cyclic injection test on day 2 was intended to re-assess the fracture opening pressure by updating and extending the step-rate test result from the previous stimulation. Progressively increasing 2-h cycles were planned to be injected starting with 2 l/s, ending with 8 l/s and using a base rate of 1 l/s and 1 l/s steps of pressure increase.

Day 3 (progressive cyclic pulse injection)

On day 3, the same volume was planned to be injected as on day 2 with same injection schedule, except that ten short-term (6 min) cycles with alternating injection rates between 1 l/s above and 1 l/s below the equivalent constant injection rate of day 2 are added on top of each HIR phase. This is done for hydraulic pulse testing analysis (Fokker et al. 2017), for evaluating the technical feasibility and to study the differences between cyclic progressive injection and cyclic progressive pulse injection.

Day 4 (shut-in)

To determine the effect of shut-in on the seismicity and pressure development, to evaluate the result of the first 3 days and to adapt the main stimulation schedule, the well was planned to be shut-in for at least 1 day.

Days 5–8 (cyclic stimulation treatment)

The number of days for the main stimulation treatment is limited by the maximum injectable net volume of 2000 m³ and the actual flow rates applied during the treatment. Also the injection schedule of each day needs to be re-evaluated on a daily basis. If no changes are necessary, the same injection schedule is repeated every day. It includes four cycles with progressively increasing flow rates from 4 to 10 l/s in steps of 2 l/s to re-evaluate the fracture opening pressure, to determine at which flow rate this pressure is reached and to ensure slow pressure increase. This is followed by three injection cycles that are a repetition of the fourth cycle to limit the pressures to values slightly above the fracture opening pressure. During the low-rate phases, the injection rate is reduced to half of the high-rate phases to keep the pressure above the fracture closure pressure during the repeated main stimulation cycles and to reduce the abrupt pressure reduction

during the progressively increasing flow rate stages. After the last cycle, the flow rate is reduced to the base rate of 1 l/s overnight to slowly close the fractures and relax the reservoir while the seismicity triggered during the day can diminish.

Day 9—pressure reduction and shut-in

After the last day of cyclic stimulation, the pressure is slowly reduced below the fracture closure pressure. Injection is carried out at the base rate of 1 l/s for as long as it takes for the pressure to reduce below the fracture closure pressure. Once the pressure is reduced sufficiently, the well is shut-in. If the pressure cannot be reduced enough flow back is performed.

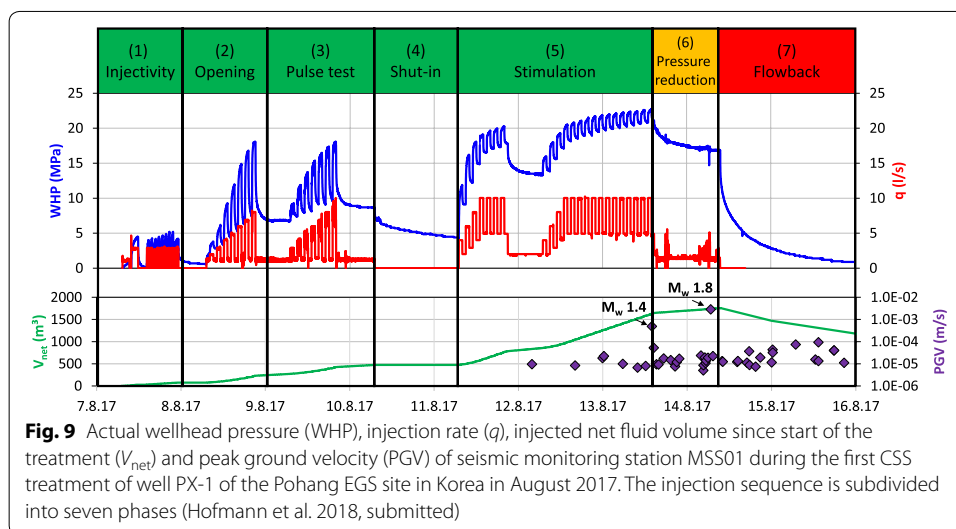
Day 10—injection tests

If seismicity allows and the pressure is reduced such that 3 l/s injection would not re-open the fractures, the same injection tests that were performed on day 1 should be repeated to evaluate the effect of the stimulation on the injectivity.

Results of CSS treatment in August 2017 in Pohang

The results of the CSS treatment in August 2017 in Pohang are shortly summarized here to show how the concept was applied for the first time in the field. Wellhead pressures, flow rates and seismic events that were registered in near real time are given in Fig. 9 throughout all phases of the treatment. A detailed presentation and analysis of the results are provided by Hofmann et al. (submitted).

The treatment is divided into seven phases. In Phase 1, the initial injectivity was determined to be ~0.5 l/s/MPa. In Phase 2, the fracture opening pressure was determined to lie between 15 and 17 MPa. In Phase 3, the same injection scheme as in Phase 2 was repeated, but with STCs on top of the progressively increasing injection rate. This was the only phase where STCs were applied. After these initial tests, 1 day of shut-in (Phase 4) followed with no seismic response. The first part of the main stimulation treatment



(Phase 5) was performed with 1-day LTC. A second part followed with an extended LTC because still no seismicity was observed before the BIR phase of the first part. During a HIR phase, a seismic event with M_w 1.4 (later revised to M_w 1.2) occurred, leading to an orange traffic-light alert with pressure reduction by flow rate reduction to BIR (Phase 6). During BIR, a M_w 1.8 (later revised to M_w 1.9) occurred, leading to a red traffic-light alert with immediate flowback and later artificial pumping to produce back all of the injected fluid volume (Phase 7). During this time, the magnitude never reached M_w 1.9 again. While the injectivity was found to be pressure dependent, no significant sustainable hydraulic performance increase could be achieved by the treatment, possibly due to the short duration and volume of the treatment, and potential closure of the stimulated fractures at low pressures.

Overall, the presented procedure was able to limit the maximum magnitude at least for the investigated time frame. Compared to the previous continuous injection treatment performed in December 2016 in the same well, the maximum magnitude was only M_w 1.8 (later revised to M_w 1.9) compared to M_L 2.3. However, a direct comparison of these two treatments is difficult and one dataset is insufficient to prove the concept. For more details about the Pohang CSS treatment in August 2017, the reader is referred to Hofmann et al. (submitted).

Discussion

The proposed stimulation concept is based on past experiences from cyclic mechanical loading experiments and cyclic injection experiments on different scales and numerical simulations, which indicate a reduction in seismicity compared to conventional constant injection procedures. Although, some explanations were proposed for the underlying mechanisms (e.g., Zang et al. 2013, 2017, 2018 and in this manuscript), it is necessary to further investigate the processes leading to these observations at different scales. Therefore, the different components of the CSS concept may currently be seen as optional modules. Future research will clarify which of these components are the most important, if some of them need to be adapted or revised, if more components need to be added, and how they can be optimized. Future studies should also focus on methods to better constrain the different treatment parameters and thresholds.

LMEs may still occur depending on the geological conditions which have to be understood beforehand. After risk evaluation, it should be decided whether the CSS concept can reduce the risk of inducing a magnitude of a certain size sufficiently. For this, especially structural geological knowledge, stress field directions and magnitudes and hydraulic behavior are essential to assess the risk of significant slip of a large area of a critically stressed fault due to fluid pressure increase or poroelastic stress transfer.

If the initial shear stress is sufficiently high, once a rupture initiates, it may propagate over large fault patches and the rupture may “jump” between neighboring faults. In that case, the maximum magnitude is controlled by tectonic factors such as stress conditions and fault dimension (e.g., Dietrich et al. 2015; Norbeck and Horne 2018). Over a wide range of subcritical shear stresses, induced earthquake ruptures are able to propagate only over a sufficiently pressurized portion of the fault. In that case, the maximum magnitude is likely limited by extent of the pressurized zone (Norbeck and Horne 2018), which depends on the injection parameters and can hence better be controlled. Additionally,

Norbeck and Horne (2018) argue that faults with strong rate-weakening friction behavior tend to behave as runaway ruptures independent of stress conditions or extent of pressure perturbation. Another point to consider is that long-term (months–years) and far field (kilometers) effects of cyclic and continuous injection treatments are not much different due to pressure diffusion, which “smears” the hydraulic response. Therefore, seismic risk reduction may sometimes not be effectively achieved by different injection schemes, but rather by improving the knowledge about stress field, structural geology and hydraulic setting of the subsurface system and appropriate siting of the wells.

The presented CSS injection schedule for the Pohang EGS project was applied with some changes due to pressure and seismicity development in August 2017 in the field. During and sometime after this hydraulic stimulation treatment, no seismic events with magnitude above 2.0 were monitored in the vicinity of the Pohang site during the stimulation campaign, which indicates that the proposed concept can achieve its major goal—limiting the maximum magnitude below a certain threshold. Longer term behavior is difficult to judge since multiple stimulation treatments and other site operations were performed before and after the CSS test.

On 15 November 2017, a M_w 5.5 earthquake occurred in the vicinity of the EGS site (KMA 2018). Currently, investigations are underway to learn whether and how EGS site operations could be related to this event (Grigoli et al. 2018; Kim et al. 2018b).

Conclusions

A cyclic soft stimulation concept is introduced as a potential method to mitigate fluid injection-induced large magnitude seismic events related to hydraulic stimulation treatments. The cyclic soft stimulation concept consists of three different types of injection cycles acting at different time scales and a traffic light system that distinguishes between actions to be taken during high-rate injection stages and low-rate injection stages, and dictates the injection procedure for the following injection phase. Additional components of this concept are the limitation of the maximum injected net volume based on a site-specific volume–magnitude relation, limitation of the maximum pressures, slow pressure changes, and flow back instead of shut-in. These components are based on experimental observations at different scales.

It is recommended to perform cyclic soft stimulation treatments in conjunction with a multi-stage injection concept and sufficient knowledge about nearby faults and their criticality in the stress field to effectively lower the risk of fluid-injection-induced large seismic events. To prove or reject different aspects of the proposed concept and to investigate the underlying processes in more detail, more well-documented experiments at different scales are required.

For a first field test, the concept was explicitly developed for the Pohang EGS site with a net volume limited to 2000 m³, flow rates limited to 10 l/s and wellhead pressures limited to 25 MPa. Long-term (1 day), medium-term (1 h), and short-term (6 min) cycles were adopted and a traffic light system was used to limit the magnitude of induced seismic events below 2.0. During stimulation and flowback, a maximum moment magnitude of M_w 1.8 (later revised to M_w 1.9) was observed, which was below the target threshold of M_w 2.0 and below the maximum magnitude from the previous continuous injection treatment in the same well of M_L 2.3 (Kim et al. 2017).

Abbreviations

a : constant of Gutenberg–Richter law; A : area of a fracture of fault that ruptures during an earthquake; b : constant of Gutenberg–Richter law; BIR: base injection rate; C : cohesion; c_t : total compressibility; CSS: cyclic soft stimulation; D_n : average normal displacement of a fracture or fault due to tensile opening; D_s : average shear displacement on a fracture or fault during rupture; EGS: enhanced geothermal system; FOP: fracture opening pressure; G : shear modulus; h : reservoir thickness; HIR: high injection rate; k : permeability; LIR: low injection rate; LME: large magnitude seismic event; LTC: long-term cycle; M_0 : seismic moment; M_w : seismic moment magnitude; M_L : local seismic magnitude; $M_{w,max}$: critical moment magnitude that is to be avoided; ΔM_w : difference in seismic magnitude between stages in the traffic light system; MTC: medium-term cycle; N : number of earthquakes with magnitude greater than or equal to M_w ; P : fluid pressure; PGV: peak ground velocity; q : injection rate; r : radial distance; r_f : rupture radius of a circular rupture plane; STC: short-term cycle; t : time; TLS: traffic light system; V : injected fluid volume; V_g : reservoir volume affected by pore pressure disturbance; V_{net} : injected net fluid volume; WHP: wellhead pressure; β : fracture or fault orientation; η : diffusivity; μ : fluid viscosity; μ_s : coefficient of static friction; σ_1 : maximum principal stress; σ_3 : minimum principal stress; σ_n : normal stress; σ' : effective stress; τ : shear stress; τ_f : frictional shear strength; $\Delta\tau$: shear stress drop; ϕ : porosity; ω : storativity.

Authors' contributions

HH wrote the manuscript, prepared the figures and developed the presented CSS concept. GZ revised the manuscript and developed the presented CSS concept. AZ revised the manuscript and developed the presented CSS concept. K-BM revised the manuscript and the CSS concept. All authors read and approved the final manuscript.

Author details

¹ Section Geothermal Energy Systems, Helmholtz Centre Potsdam GFZ German Research Centre for Geosciences, Telegrafenberg, 14473 Potsdam, Germany. ² Section Seismic Hazard and Risk Dynamics, Helmholtz Centre Potsdam GFZ German Research Centre for Geosciences, Telegrafenberg, 14473 Potsdam, Germany. ³ Department of Energy Resources Engineering, Seoul National University, 1 Gwanak-ro, Gwanak-gu, Seoul 08826, Republic of Korea.

Acknowledgements

The authors are grateful for the funding received from the European Union's Horizon 2020 research and innovation programme under Grant agreement No. 691728 (DESTRESS). This work was also supported by the Korea–EU Joint Research Support Program of the National Research Foundation of Korea (NRF) through a Grant (No. NRF-2015K1A3A7A03074226) funded by the Korean Government's Ministry of Science and ICT.

Competing interests

The authors declare that they have no competing interests.

Availability of data and materials

Data sharing is not applicable to this article as no new dataset was generated or analyzed during the current study. The data shown in Fig. 9 will be made available in conjunction with the following publication: Hofmann H, Zimmermann G, Farkas M, Huenges E, Zang A, Leonhardt M, Kwiatek G, Martinez-Garzon P, Bohnhoff M, Min K-B, Fokker P, Westaway R, Bethmann F, Meier P, Yoon KS, Choi JW, Lee TJ, and Kim KY (submitted), First field application of cyclic soft stimulation at the Pohang Enhanced Geothermal System site in Korea, submitted to *Geophysical Journal International*.

Funding

Hannes Hofmann was funded by the European Union's Horizon 2020 research and innovation programme under Grant agreement No. 691728 (DESTRESS). Ki-Bok Min was funded by the Korea–EU Joint Research Support Program of the National Research Foundation of Korea (NRF) through a Grant (No. NRF-2015K1A3A7A03074226) funded by the Korean Government's Ministry of Science and ICT.

Publisher's Note

Springer Nature remains neutral with regard to jurisdictional claims in published maps and institutional affiliations.

Received: 13 June 2018 Accepted: 21 November 2018

Published online: 05 December 2018

References

- Bao X, Eaton DW. Fault activation by hydraulic fracturing in western Canada. *Science*. 2016;354:1406–9. <https://doi.org/10.1126/science.aag2583>.
- Bachmann CE, Wiemer S, Woessner J, Hainzl S. Statistical analysis of the induced Basel 2006 earthquake sequence: introducing a probability-based monitoring approach for Enhanced Geothermal Systems. *Geophys J Int*. 2011;186:793–807. <https://doi.org/10.1111/j.1365-246X.2011.05068.x>.
- Bachmann CE, Wiemer S, Goertz-Allmann BP, Woessner J. Influence of pore pressure on the event-size distribution of induced earthquakes. *Geophys Res Lett*. 2012;39:L09302. <https://doi.org/10.1029/2012GL051480>.
- Baisch S, Harjes H-P. A model for fluid-injection-induced seismicity at the KTB, Germany. *Geophys J Int*. 2003;152(1):160–70. <https://doi.org/10.1046/j.1365-246X.2003.01837.x>.
- Baisch S, Weidler R, Vörös R, Wyborn D, de Graaf L. Induced seismicity during the stimulation of a geothermal HFR reservoir in the Cooper Basin, Australia. *Bull Seismol Soc Am*. 2006;96(2):2242–56. <https://doi.org/10.1785/0120050255>.
- Barth A, Wenzel F, Langenbruch C. Probability of earthquake occurrence and magnitude estimation in the post shut-in phase of geothermal projects. *J Seismol*. 2013;17:5–11. <https://doi.org/10.1007/s10950-011-9260-9>.
- BC Oil and Gas Commission. Investigation of observed seismicity in the Horn River Basin. Technical report. 2012. <https://www.bcogc.ca/investigation-observed-seismicity-horn-river-basin>. Accessed 03 Aug 2018.

- Blöcher G, Cacace M, Jacquey AB, Zang A, Heibach O, Hofmann H, Kluge C, Zimmermann G. Evaluating micro-seismic events triggered by reservoir operations at the geothermal site of Groß Schönebeck (Germany). *Rock Mech Rock Eng*. 2018. <https://doi.org/10.1007/s00603-018-1521-2>.
- Bormann P, Di Giacomo D. The moment magnitude M_w and the energy magnitude M_e : common roots and differences. *J Seismol*. 2011;15(2):411–27. <https://doi.org/10.1007/s10950-010-9219-2>.
- Bommer JJ, Oates S, Cepeda JM, et al. Control of hazard due to seismicity induced by a hot fractured rock geothermal project. *Eng Geol*. 2006;83:287–306. <https://doi.org/10.1016/j.enggeo.2005.11.002>.
- Bommer JJ, Crowley H, Pinho R. A risk-mitigation approach to the management of induced seismicity. *J Seismol*. 2015;19:623–46. <https://doi.org/10.1007/s10950-015-9478-z>.
- Bunger AP, McLennan J, Jeffrey R. Effective and sustainable hydraulic fracturing. Rijeka: InTech; 2013.
- Cerfontaine B, Collin F. Cyclic and fatigue behavior of rock materials: review, interpretation and research perspectives. *Rock Mech Rock Eng*. 2017. <https://doi.org/10.1007/s00603-017-1337-5>.
- Cesca S, Dost B, Oth A. Preface to the special issue “Triggered and induced seismicity: probabilities and discrimination”. *J Seismol*. 2013;17:1–4. <https://doi.org/10.1007/s10950-012-9338-z>.
- Charl y J, Cuenot N, Dorbath L, et al. Large earthquakes during hydraulic stimulations at the geothermal site of Soultz-sous-Forets. *Int J Rock Mech Min*. 2007;44:1091–105. <https://doi.org/10.1016/j.ijrmm.2007.06.003>.
- Cipolla CL, Wright CA. State-of-the-Art in hydraulic fracture diagnostics. In: SPE Asia Pacific Oil and Gas Conference and Exhibition, 16–18 October 2000, SPE 64434. Brisbane, Australia. <https://doi.org/10.2118/64434-MS>.
- Clarke H, Eisner L, Styles P, Turner P. Felt seismicity associated with shale gas hydraulic fracturing: the first documented example in Europe. *Geophys Res Lett*. 2014;41(23):8308–14. <https://doi.org/10.1002/2014GL062047>.
- Cornet FH. The relationship between seismic and aseismic motions induced by forced fluid injections. *Hydrogeol J*. 2012;20:1463–6. <https://doi.org/10.1007/s10040-012-0901-z>.
- Cornet FH. Seismic and aseismic motions generated by fluid injections. *Geomech Energy Environ*. 2016;5:42–54. <https://doi.org/10.1016/j.gete.2015.12.003>.
- Davies R, Foulger G, Bindley A, Styles P. Induced seismicity and hydraulic fracturing for the recovery of hydrocarbons. *Mar Pet Geol*. 2013;45:171–85. <https://doi.org/10.1016/j.marpetgeo.2013.03.016>.
- Deichmann N, Giardini D. Earthquakes induced by the stimulation of an enhanced geothermal system below Basel (Switzerland). *Seismol Res Lett*. 2009;80:784–98. <https://doi.org/10.1785/gssrl.80.5.784>.
- Diaz M, Jung SG, Zhuang L, Kim KY, Zimmermann G, Hofmann H, Zang A, Stephansson O, Min K-B. Hydraulic, Mechanical and seismic observations during hydraulic fracturing by cyclic injection on pocheon granite. In: 10th asian rock mechanics symposium. Singapore, 29 October–3 November. 2018a.
- Diaz M, Jung SG, Zhuang L, Kim KY. Comparison of acoustic emission activity in conventional and cyclic hydraulic fracturing in cubic granite samples under tri-axial stress state. In: 52nd US rock mechanics/geomechanics symposium, Seattle, WA, USA, 17–20 June. 2018b. ARMA 18-1160.
- Dietrich JH, Richards-Dinger KB, Kroll KA. Modeling injection-induced seismicity with the physics-based earthquake simulator RSQSim. *Seismol Res Lett*. 2015;86(4):1102–9. <https://doi.org/10.1785/0220150057>.
- Downie R, Kronenberger E, Maxwell SC. Using microseismic source parameters to evaluate the influence of faults on fracture treatments: a geophysical approach to interpretation. In: SPE annual technical conference and exhibition, SPE 134772. Florence, Italy, 19–22 September. 2010.
- Eaton DW, Maghsoudi S. 2b... or not 2b? Interpreting magnitude distributions from microseismic catalogs. *First Break*. 2015;33(10):79–86.
- Economides MJ, Nolte KG. Reservoir stimulation. 3rd ed. Chichester: Wiley; 2000.
- Economides MJ, Martin T. Modern fracturing: Enhancing natural gas production. Houston: ET Publishing; 2007.
- Ellsworth WL. Injection-induced earthquakes. *Science*. 2013;341:12259421–7. <https://doi.org/10.1126/science.1225942>.
- Erarslan N, Alehossein H, Williams DJ. Tensile fracture strength of Brisbane Tuff by static and cyclic loading tests. *Rock Mech Rock Eng*. 2014;47:1135–51. <https://doi.org/10.1007/s00603-013-0469-5>.
- Fatemi A, Yang L. Cumulative fatigue damage and life prediction theories: a survey of the state of the art for homogeneous materials. *Int J Fatigue*. 1998;20:9–34. [https://doi.org/10.1016/S0142-1123\(97\)00081-9](https://doi.org/10.1016/S0142-1123(97)00081-9).
- Fokker PA, Borello EES, Viberti D. Harmonic pulse testing for well and reservoir characterization. In: 9th EAGE conference and exhibition, Paris, France, 12–15 June. 2017. SPE-185815-MS.
- French ME, Zhu W, Banker J. Fault slip controlled by stress path and fluid pressurization rate. *Geophys Res Lett*. 2016;43(9):4330–9. <https://doi.org/10.1002/2016GL068893>.
- Galis M, Ampuero JP, Mai PM, Cappa F. Induced seismicity provides insight into why earthquake ruptures stop. *Sci Adv*. 2017;3(12):eaap7528. <https://doi.org/10.1126/sciadv.aap7528>.
- Ghamgosar M, Erarslan N. Experimental and numerical studies on development of fracture process zone (FPZ) in rocks under cyclic and static loadings. *Rock Mech Rock Eng*. 2016;49:893–908. <https://doi.org/10.1007/s00603-015-0793-z>.
- Goodfellow SD, Nasser MHB, Maxwell SC, Young RP. Hydraulic fracture energy budget: insights from the laboratory. *Geophys Res Lett*. 2015;42(9):3179–87. <https://doi.org/10.1002/2015gl063093>.
- Grant MA, Clearwater J, Quinao J, Bixley PF, Brun ML. Thermal stimulation of geothermal wells: a review of field data. In: Thirty-eight workshop on geothermal reservoir engineering, Stanford, California, February 11–13. 2013. SGP-TR-198.
- Grigoli F, Cesca S, Rinaldi AP, Manconi A, L pez-Comino JA, Clinton JF, Westaway R, Cauzzi C, Dahm T, Wiemer S. The November 2017 M_w 5.5 Pohang earthquake: a possible case of induced seismicity in South Korea. *Science*. 2018. <https://doi.org/10.1126/science.aat2010>.
- Guglielmi Y, Cappa F, Amitrano D. High-definition analysis of fluid-induced seismicity related to the mesoscale hydromechanical properties of a fault zone. *Geophys Res Lett*. 2008;35:L06306. <https://doi.org/10.1029/2007GL033087>.
- Gutenberg R, Richter CF. Frequency of Earthquakes in California. *Bull Seismol Soc Am*. 1944;34(4):185–8.
- Hanks TC, Kanamori H. A moment magnitude scale. *J Geophys Res*. 1979;84(B5):2348–50. <https://doi.org/10.1029/JB084iB05p02348>.

- Häring MO, Schanz U, Ladner F, Dyer BC. Characterisation of the Basel 1 enhanced geothermal system. *Geothermics*. 2008;37:469–95. <https://doi.org/10.1016/j.geothermics.2008.06.002>.
- Heap MJ, Faulkner DR. Quantifying the evolution of static elastic properties as crystalline rock approaches failure. *Int J Rock Mech Min Sci*. 2008;45:564–73. <https://doi.org/10.1016/j.ijrmms.2007.07.018>.
- Heap MJ, Vinciguerra S, Meredith PG. The evolution of elastic moduli with increasing crack damage during cyclic stressing of a basalt from Mt. Etna volcano. *Tectonophysics*. 2009;471(1–2):153–60. <https://doi.org/10.1016/j.tecto.2008.10.004>.
- Heap M, Faulkner D, Meredith P, Vinciguerra S. Elastic moduli evolution and accompanying stress changes with increasing crack damage: implications for stress changes around fault zones and volcanoes during deformation. *Geophys J Int*. 2010;183(1):225–36. <https://doi.org/10.1111/j.1365-246X.2010.04726.x>.
- Hofmann H, Babadagli T, Zimmermann G. Hot water generation for oil sands processing from enhanced geothermal systems: process simulation for different hydraulic fracturing scenarios. *Appl Energy*. 2014;113:524–47. <https://doi.org/10.1016/j.apenergy.2013.07.060>.
- Hofmann H, Babadagli T, Yoon JS, Blöcher G, Zimmermann G. A hybrid discrete/finite element modeling study of complex hydraulic fracture development for enhanced geothermal systems (EGS) in granitic basements. *Geothermics*. 2016a;64:362–81. <https://doi.org/10.1016/j.geothermics.2016.06.016>.
- Hofmann H, Blöcher G, Milsch H, Babadagli T, Zimmermann G. Transmissivity of aligned and displaced tensile fractures in granitic rocks during cyclic loading. *Int J Rock Mech Mining Sci*. 2016b;87:69–84. <https://doi.org/10.1016/j.ijrmms.2016.05.011>.
- Hofmann H, Zimmermann G, Zang A, Yoon JS, Stephansson O, Kim KY, Zhuang L, Diaz M, Min K-B. Comparison of cyclic and constant fluid injection in granitic rock at different scales. In: 52nd US rock mechanics/geomechanics symposium. Seattle, Washington, 17–20 June 2018. 2018. ARMA 18-691.
- Hofmann H, Zimmermann G, Farkas M, Huenges E, Zang A, Leonhardt M, Kwiatek G, Martinez-Garzon P, Bohnhoff M, Min K-B, Fokker P, Westaway R, Bethmann F, Meier P, Yoon KS, Choi JW, Lee TJ, Kim KY (submitted). First field application of cyclic soft stimulation at the Pohang Enhanced Geothermal System site in Korea. *Geophys J Int*.
- Huenges E, Ledru P. *Geothermal energy systems: exploration, development, and utilization*. Weinheim: Wiley-VCH; 2010.
- Inamdar A, Malpani R, Atwood K, Brook K, Erwemi A, Ogundare T, Purcell D. Evaluation of stimulation techniques using microseismic mapping in the Eagle Ford Shale. In: Tight gas completions conference, SPE 136873. San Antonio, TX, USA, 2–3 November. 2010. <https://doi.org/10.2118/136873-MS>.
- Johri M, Zoback MD. The evolution of stimulated reservoir volume during hydraulic stimulation of shale gas formations. In: Proceedings of the unconventional resources technology conference. Colorado, 12–14 August. 2013.
- Kaiser J. Untersuchungen über das Auftreten von Geräuschen beim Zugversuch. Ph.D. thesis, Fak. F. Maschinenwesen, TH München, Germany. 1950.
- Kiel OM. The Kiel process—reservoir stimulation by dendritic fracturing. *Society of Petroleum Engineers, SPE 6984*; 1977. p. 29.
- Kim MS, Yoon BJ, Lee CH, Park KG, Yoon WS, Song YH, Lee TJ. Microseismic monitoring during hydraulic stimulation in Pohang (Korea) for EGS pilot project. In: AGU fall meeting. December 11–15 2017, New Orleans. 2017.
- Kim K-I, Min K-B, Kim K-Y, Choi JW, Yoon K-S, Yoon WS, Yoon BJ, Lee TJ, Song YH. Protocol for induced microseismicity in the first enhanced geothermal systems project in Pohang, Korea. *Renew Sustain Energy Rev*. 2018a;91:1182–91. <https://doi.org/10.1016/j.rser.2018.04.062>.
- Kim K-H, Ree J-H, Kim YH, Kim S, Kang SY, Seo W. Assessing whether the 2017 M_w 5.4 Pohang earthquake in South Korea was an induced event. *Science*. 2018b. <https://doi.org/10.1126/science.aat6081>.
- KMA—Korea Meteorological Administration. 2018. http://www.weather.go.kr/weather/earthquake_volcano/report.jsp. Accessed 09 July 2018.
- Kwiatek G, Bohnhoff M, Schulze A, et al. Microseismicity induced during fluid-injection: a case study from the geothermal site at Groß Schönebeck, North German Basin. *Acta Geophys*. 2010;58:995–1020.
- Kwiatek G, Martínez-Garzón P, Plenkers K, Leonhardt M, Zang A, von Specht S, Dresen G, Bohnhoff M. Insights into complex subdecimeter fracturing processes occurring during a water injection experiment at depth in Äspö Hard Rock Laboratory, Sweden. *J Geophys Res Solid Earth*. 2018;11. <https://doi.org/10.1029/2017JB014715>.
- Lahaie F, Grasso JR. *J Geophys Res*. 1999;104(B8):17941–54. <https://doi.org/10.1029/1999JB900139>.
- Lay T, Wallace TC. *Modern global seismology*. Cambridge: Academic press; 1995. p. 521.
- Lee T, Song Y, Yoon WS. The first geothermal power generation project by Enhanced Geothermal System (EGS) in Korea. EGU General Assembly. *Geophys Res*. 2013;15:EGU2013-6728.
- Legarth BA, Huenges E, Zimmermann G. Hydraulic fracturing in a sedimentary geothermal reservoir: results and implications. *Int J Rock Mech Min Sci*. 2005;42(7–8):1028–41. <https://doi.org/10.1016/j.ijrmms.2005.05.014>.
- Majer EL, Baria R, Stark M, et al. Induced seismicity associated with enhanced geothermal systems. *Geothermics*. 2007;36:185–222. <https://doi.org/10.1016/j.geothermics.2007.03.003>.
- Majer E, Nelson J, Robertson-Tait A, Savy J, Wong I. Protocol for addressing induced seismicity associated with enhanced geothermal systems. Technical report. 2012. DOE/EE-0662.
- Majorowicz J, Hofmann H, Babadagli T. Deep geothermal heat storage under oil sands—can we use it to help oilsands industry? New EGS concept proposed. *GRC Transac*. 2013;37:173–8.
- Maxwell SC, Urbancic TI, Demerling C, Prince M. Real-Time 4D passive seismic imaging of hydraulic fracturing. 2002. SPE/ISRM 78191.
- Maxwell SC, Schemeta J, Campbell E, Quirk D. Microseismic deformation rate monitoring. In: SPE annual technical conference and exhibition, SPE 116596. Denver, CO, USA, 21–24 September. 2008.
- Maxwell SC. Unintentional seismicity induced by hydraulic fracturing. *CSEG Rec*. 2013;38(8):40–9.
- Maxwell SC, Zhang F, Damjanac B. Geomechanical modeling of induced seismicity resulting from hydraulic fracturing. *Lead Edge*. 2015;34(6):678–83.
- McClure MW, Horne RN. Correlations between formation properties and induced seismicity during high pressure injection into granitic rock. *Eng Geol*. 2014;175:74–80. <https://doi.org/10.1016/j.enggeo.2014.03.015>.

- McGarr A. Maximum magnitude earthquakes induced by fluid injection. *J Geophys Res Solid Earth*. 2014;119:1008–19. <https://doi.org/10.1002/2013JB010597>.
- Meier PM, Rodríguez A, Bethmann F. Lessons learned from Basel: New EGS projects in Switzerland using multistage stimulation and a probabilistic traffic light system for the reduction of seismic risk. In: Proceedings world geothermal congress. Melbourne, Australia, 19–25 April. 2015.
- Mena B, Wiemer S, Bachmann C. Building robust models to forecast induced seismicity related to geothermal reservoir enhancement. *Bull Seismol Soc Am*. 2013;103:383–93. <https://doi.org/10.1785/0120120102>.
- Mukuhira Y, Dinske C, Asanuma H, Ito T, Häring MO. Pore pressure behavior at the shut-in phase and causality of large induced seismicity at Basel, Switzerland. *J Geophys Res Solid Earth*. 2017;122:411–35. <https://doi.org/10.1002/2016JB013338>.
- National Research Council—NRC. Induced seismicity potential in energy technologies. Washington, DC: The National Academies Press; 2013. <https://doi.org/10.17226/13355>.
- Norbeck JH, Horne RN. Maximum magnitude of injection-induced earthquakes: a criterion to assess the influence of pressure migration along faults. *Tectonophysics*. 2018;733:108–18. <https://doi.org/10.1016/j.tecto.2018.01.028>.
- Oprsal I, Eisner L. Cross-correlation—an objective tool to indicate induced seismicity. *Geophys J Int*. 2014;196(3):1536–43. <https://doi.org/10.1093/gji/ggt501>.
- Park S, Xie L, Kim K-I, Kwon S, Min K-B, Choi J, Yoon W-S, Song Y. First hydraulic stimulation in fractured geothermal reservoir in Pohang PX-2 well. In: 42nd workshop on geothermal reservoir engineering. Stanford, California, February 13–15. 2017a. SGP-TR-212.
- Park S, Kim K-I, Xie L, Yoo H, Min K-B, Choi J, Yoon W-S, Yoon K, Song Y, Lee TJ, Kim KY. Hydraulic stimulation in fractured geothermal reservoir in Pohang PX-1 well. YSRM 2017 & NDRMGE. Jeju, Korea, May 10–13. 2017b; pp. 373–4.
- Patel S, Sondergeld C, Rai C. Laboratory studies of cyclic injection hydraulic fracturing. In: SEG international exposition and 86th annual meeting. Dallas, TX, USA, 16–21 October. 2016.
- Raleigh CB, Healy JH, Bredehoeft JD. An experiment in earthquake control at Rangely, Colorado. *Science*. 1976;191(4233):1230–7. <https://doi.org/10.1126/science.191.4233.1230>.
- Sagar RV, Rao MVMS. An experimental study on loading rate effect on acoustic emission based *b*-values related to reinforced concrete fracture. *Constr Build Mater*. 2014;70:460–72. <https://doi.org/10.1016/j.conbuildmat.2014.07.076>.
- Sano O, Ito I, Terada M. Influence of strain rate on dilatancy and strength of Oshima granite under uniaxial compression. *J Geophys Res*. 1981;86:9299–311. <https://doi.org/10.1029/JB086iB10p09299>.
- Sano O, Terada M, Ehara S. A study on the time-dependent microfracturing and strength of Oshima granite. *Tectonophysics*. 1982;84:343–62. [https://doi.org/10.1016/0040-1951\(82\)90167-6](https://doi.org/10.1016/0040-1951(82)90167-6).
- Schulz CH. Earthquakes and friction laws. *Nature*. 1998;391:37–42.
- Shapiro SA, Dinske C. Scaling of seismicity induced by nonlinear fluid-rock interaction. *J Geophys Res*. 2009;114:B09307. <https://doi.org/10.1029/2008JB006145>.
- Shapiro SA, Dinske C, Kummerow J. Probability of a given-magnitude earthquake induced by a fluid injection. *Geophys Res Lett*. 2007;34:L22314. <https://doi.org/10.1029/2007GL031615>.
- Shapiro SA, Dinske C, Langenbruch C, Wenzel F. Seismogenic index and magnitude probability of earthquakes induced during reservoir stimulations. *Lead Edge*. 2010;29(3):304–409. <https://doi.org/10.1190/1.3353727>.
- Song Y, Lee TJ, Jeon J, Yoon WS. Background and progress of the Korean EGS pilot project. In: Proceedings world geothermal congress. Melbourne, Australia, 19–25 April. 2015.
- Stephansson O, Semikova H, Zimmermann G, Zang A. Laboratory pulse test of hydraulic fracturing on granitic sample cores from Äspö HRL. Sweden: *Rock Mech Rock Eng*; 2018. <https://doi.org/10.1007/s00603-018-1421-5>.
- Tester JW, et al. The future of geothermal energy: Impact of Enhanced Geothermal Systems (EGS) on the United States in the 21st Century. Cambridge: MIT; 2006.
- Tiancheng L, Baoshan G, Yuzhong Y, Haifeng F, Yun X, Yunzhi L. Laboratory study of hydraulic fracturing in cyclic injection. In: 52nd US Rock mechanics/geomechanics symposium. Seattle, WA, USA, 17–20 June. 2018. ARMA 18-047.
- Vlcek J, Eisner L, Stabile TA, Telesca L. Temporal relationship between injection rates and induced seismicity. *Pure Appl Geophys*. 2017. <https://doi.org/10.1007/s00024-017-1622-y>.
- Vogler D, Amann F, Bayer P, Elsworth D. Permeability evolution in natural fractures subject to cyclic loading and gouge formation. *Rock Mech Rock Eng*. 2016;49:3463–79. <https://doi.org/10.1007/s00603-016-1022-0>.
- Wang X, Wen Z, Jiang Y, Huang H. Experimental study on mechanical and acoustic emission characteristics of rock-like material under non-uniformly distributed loads. *Rock Mech Rock Eng*. 2018;51:729–45. <https://doi.org/10.1007/s00603-017-1363-3>.
- Wenzel F. Fluid-induced seismicity: comparison of rate- and state- and critical pressure theory. *Geotherm Energy*. 2017;5:5. <https://doi.org/10.1186/s40517-017-0063-2>.
- Wilson MP, Worrall F, Davies RJ, Almond S. Fracking: How far from faults? *Geomech Geophys Geo-Energy Geo-Resour*. 2018;1:1. <https://doi.org/10.1007/s40948-018-0081-y>.
- Yoon JS, Zimmermann G, Zang A. Discrete element modeling of cyclic rate fluid injection at multiple locations in naturally fractured reservoirs. *Int J Rock Mech Min Sci*. 2015;74:15–23. <https://doi.org/10.1016/j.ijrmms.2014.12.003>.
- Zang A, Yoon JS, Stephansson O, Heidbach O. Fatigue hydraulic fracturing by cyclic reservoir treatment enhances permeability and reduces induced seismicity. *Geophys J Int*. 2013;195:1282–7. <https://doi.org/10.1093/gji/ggt301>.
- Zang A, Oye V, Jousset P, Deichmann N, Gritto R, McGarr A, Majer E, Bruhn D. Analysis of induced seismicity in geothermal reservoirs—an overview. *Geothermics*. 2014;52:6–21. <https://doi.org/10.1016/j.geothermics.2014.06.005>.
- Zang A, Stephansson O, Stenberg L, et al. Hydraulic fracture monitoring in hard rock at 410 m depth with an advanced fluid-injection protocol and extensive sensor array. *Geophys J Int*. 2017;208:790–813. <https://doi.org/10.1093/gji/ggw430>.
- Zang A, Zimmermann G, Hofmann H, Stephansson O, Min KB, Kim KY. How to reduce fluid-injection induced seismicity. *Rock Mech Rock Eng*. 2018. <https://doi.org/10.1007/s00603-018-1467-4>.
- Zhou Z-L, Zhang G-Q, Dong H-R, Liu Z-B, Nie Y-X. Creating a network of hydraulic fractures by cyclic pumping. *Int J Rock Mech Min Sci*. 2017;97:52–63. <https://doi.org/10.1016/j.ijrmms.2017.06.009>.

- Zhuang L, Kim KY, Jung SG, et al. Laboratory study on cyclic hydraulic fracturing of Pocheon Granite in Korea. In: 50th US Rock mechanics/geomechanics symposium. Houston, TX, USA, 26–29 June. 2016.
- Zhuang L, Kim KY, Jung SG, et al. Laboratory evaluation of induced seismicity reduction and permeability enhancement effects of cyclic hydraulic fracturing. In: 51st US rock mechanics/geomechanics symposium. San Francisco, CA, USA 25–28 June. 2017.
- Zhuang L, Kim KY, Jung SG, Diaz M, Min K-B, Park S, Zang A, Stephansson O, Zimmermann G, Yoon JS. Cyclic hydraulic fracturing of cubic granite samples under triaxial stress state with acoustic emission, injectivity and fracture measurements. In: 52nd US rock mechanics/geomechanics symposium. Seattle, WA, USA, 17–20 June. 2018. ARMA 18-297.
- Zimmermann G, Hofmann H, Babadagli T, et al. Multi-fracturing and cyclic hydraulic stimulation scenarios to develop Enhanced Geothermal Systems—feasibility and mitigation strategies to reduce seismic risk. In: Proceedings world geothermal congress. Melbourne, Australia, 19–25 April. 2015.
- Zimmermann G, Zang A, Stephansson O, Klee G, Semiková H. Permeability enhancement and fracture development of hydraulic in situ experiments in the Åspö Hard Rock Laboratory. Sweden: Rock Mech Rock Eng; 2018. <https://doi.org/10.1007/s00603-018-1499-9>.
- Zoback MD. Reservoir geomechanics. Cambridge: Cambridge University Press; 2010. ISBN 978-0-521-77069-9.

Submit your manuscript to a SpringerOpen[®] journal and benefit from:

- ▶ Convenient online submission
- ▶ Rigorous peer review
- ▶ Open access: articles freely available online
- ▶ High visibility within the field
- ▶ Retaining the copyright to your article

Submit your next manuscript at ▶ [springeropen.com](https://www.springeropen.com)
